DOI: 10.1002/cmdc.201402292

Design and Synthesis of N-Acylated Aza-Goniothalamin Derivatives and Evaluation of Their in vitro and in vivo Antitumor Activity

Rosimeire Coura Barcelos,[a] Julio Cezar Pastre,[a] Débora Barbosa Vendramini-Costa,[a, b] Vanessa Caixeta,[a] Giovanna Barbarini Longato,[b, c] Paula Araújo Monteiro,[b, c] João Ernesto de Carvalho,[b, c] and Ronaldo Aloise Pilli*[a]

Herein we describe the synthesis of a focused library of compounds based on the structure of goniothalamin (**1**) and the evaluation of the potential antitumor activity of the compounds. N-Acylation of aza-goniothalamin (**2**) restored the in vitro antiproliferative activity of this family of compounds. 1-(*E*)-But-2-enoyl-6-styryl-5,6-dihydropyridin-2(1*H*)-one (**18**) displayed enhanced antiproliferative activity. Both goniothalamin (**1**) and derivative **18** led to reactive oxygen species generation in PC-3 cells, which was probably a signal for caspase-dependent apoptosis. Treatment with derivative **18** promoted Annexin V/7-aminoactinomycin D double staining, which indicated apoptosis, and also led to G_2/M cell-cycle arrest. In vivo studies in Ehrlich ascitic and solid tumor models confirmed the antitumor activity of goniothalamin (**1**), without signs of toxicity. However, derivative **18** exhibited an unexpectedly lower in vivo antitumor activity, despite the treatments being administered at the same site of inoculation. Contrary to its in vitro profile, aza-goniothalamin (**2**) inhibited Ehrlich tumor growth, both on the ascitic and solid forms. Our findings highlight the importance of in vivo studies in the search for new candidates for cancer treatment.

1. Introduction

Cancer is a group of diseases characterized by uncontrolled growth and division of cells, which are able to invade other tissues and organs by spreading to other parts of the body through blood and lymph vessels.[1] Despite the advances in the field of anticancer drug discovery, the statistics are noteworthy: for example, 14.1 million new cases of cancer were diagnosed worldwide in 2012, with 8.2 million deaths.[2]

Among the limitations associated with the strategies currently available for cancer treatment, the development of multidrug resistance stands as the major cause of failure as far as chemotherapy is concerned.[3] In this context, it is clear that more effective drugs that are able to overcome the resistance of tumor cells, with decreased toxicity and higher tolerability by the patients, are still needed.

Nature has been a source of medicinal products for millennia, in line with the history of humanity. Due to the improvement of methods for isolation, identification, and synthesis during the last century, many drugs have been developed from natural sources. Indeed, it is estimated that 75% of the anticancer agents used nowadays in chemotherapy are derived from natural products of different origins, including plants, microorganisms, and marine organisms.[4]

Most natural products are secondary metabolites produced for defense or communication, which are often toxic and, therefore, display potential antitumor activity.[5] In this regard, (*R*)-goniothalamin (**1**, Figure 1), a styryl lactone originally isolated from a species of *Goniothalamus* (Annonaceae), displays antiproliferative and cytotoxic activities against a variety of tumor cell lines.[6]

In view of the promising antitumor effect of goniothalamin (**1**), several studies have been performed to unveil its mode of action in tumor cells.[7a–d] Although the exact mechanism responsible for the cytotoxic and antiproliferative activities displayed by goniothalamin (**1**) is not clear yet, in vivo studies performed in a solid tumor experimental model in mice confirmed the potential of goniothalamin (**1**) as a lead compound for the development of new chemotherapeutic agents.[6e] In this context, the synthesis of goniothalamin analogues has culminated in the observation of the structural requirements for expression of the cytotoxic activity.[7e–h] From these studies, the

[a] *Dr. R. C. Barcelos,[+] Dr. J. C. Pastre,[+] Dr. D. B. Vendramini-Costa,[+] V. Caixeta, Prof. R. A. Pilli*
Departamento de Química Orgânica, Instituto de Química, Universidade Estadual de Campinas, CP 6154, 13083-970, Campinas, SP (Brazil)
E-mail: pilli@iqm.unicamp.br

[b] *Dr. D. B. Vendramini-Costa,[+] G. B. Longato, P. A. Monteiro, Prof. J. E. de Carvalho*
Divisão de Farmacologia e Toxicologia, Centro Pluridisciplinar de Pesquisas Químicas, Biológicas e Agrícolas (CPQBA), UNICAMP, CP 6171, 13083-970, Campinas, SP (Brazil)

[c] *G. B. Longato, P. A. Monteiro, Prof. J. E. de Carvalho*
Programa de Pós-graduação em Biologia Celular e Estrutural, Instituto de Biologia, UNICAMP, CP 6109, 13083-970, Campinas, SP (Brazil)

[+] *These authors contributed equally to this work.*

Supporting information for this article is available on the WWW under http://dx.doi.org/10.1002/cmdc.201402292.

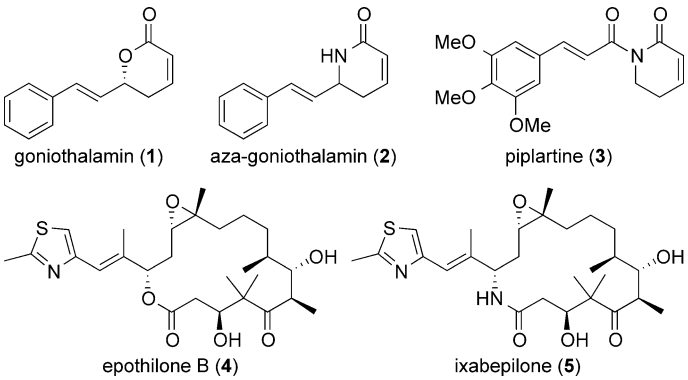

Figure 1. Chemical structures of goniothalamin (**1**), aza-goniothalamin (**2**), piplartine (**3**), epothilone B (**4**), and ixabepilone (**5**).

α,β-unsaturated δ-lactone moiety seems to be crucial, and it is ascribed to act as a Michael acceptor for cysteine residues or other nucleophiles in the biological system.[8]

Previously, a series of aza-goniothalamin derivatives was prepared and evaluated against a panel of human tumor cell lines, since the synthesis of aza analogues is a strategy used to prepare compounds with better bioavailability.[7g] Several reports have validated this approach, and ixabepilone (**5**), an aza analogue of epothilone B (**4**), stands as a good representative. In view of its increased stability due to isosteric replacement of the macrolactone by a macrolactam ring, which rendered the macrocycle less susceptible to hydrolysis, ixabepilone (**5**) was approved by the US Food and Drug Administration (FDA) for the treatment of patients with metastatic or locally advanced breast cancer that was resistant to anthracyclines and taxanes.[9]

According to our previous work, the introduction of the lactam ring completely abolished the in vitro antiproliferative activity against all cancer cell lines that were evaluated. Indeed, no compound in the aza series displayed significant cytotoxic activity, even at the highest concentration used in the assays.[7g] The loss of the in vitro activity was rationalized in terms of the much lower electron deficiency of the α,β-unsaturated δ-lactam unit having a deleterious effect on the biological profile of the aza analogues of goniothalamin (**1**).

If this hypothesis is correct, the synthesis of N-acylated aza-goniothalamin derivatives could, in principle, restore the activity of this family of compounds. From a chemical point of view, N-acylation could render the α,β-unsaturated system more prone to nucleophilic attack because the nitrogen lone pair would now be involved in cross-conjugation. Indeed, naturally occurring N-acylated α,β-unsaturated δ-lactams have been shown to display interesting antitumor activities. For example, piplartine (**3**; also known as piperlongumine), a natural alkaloid isolated from *Piper longum*, displayed selective in vitro cytotoxicity against tumor cells and also exhibited potent antitumor activity in animal models.[10] The potent cytotoxic activity of piplartine (**3**) has been related to an increased reactive oxygen species (ROS) generation in cancer cells.[10b] In addition, the ability of piplartine (**3**) to down-regulate nuclear factor-κB (NF-κB) activation was also demonstrated.[11] Moreover, piplartine (**3**) induces rapid depletion of the androgen receptor in prostate cancer cells.[12]

In view of our continuous effort to improve the antitumor profile of goniothalamin (**1**) and also to complement previous structure–activity relationship (SAR) studies, we report in this work the synthesis of a focused library of N-acylated aza-goniothalamin derivatives and their in vitro evaluation against a panel of eight human cancer cell lines: U251 (glioma), MCF-7 (breast), NCI-ADR/RES (ovarian expressing multiple-drug-resistance phenotype), 786-0 (kidney), NCI-H460 (lung non-small cells), PC-3 (prostate), OVCAR-3 (ovarian), and HT-29 (colon). We further looked at how these analogues act on the cells, with a focus on the androgen-resistant prostate cancer epithelial cell line (PC-3 cells). The most active compound (derivative **18**) was selected for in vivo studies by using the Ehrlich ascitic and solid tumor models in mice, with comparison to studies with goniothalamin (**1**) and aza-goniothalamin (**2**).

2. Results and Discussion

2.1. Chemistry

Racemic goniothalamin (**1**) was prepared in gram quantities in accordance with a previously described methodology from our group, except for the use of allylmagnesium bromide in substitution for the enantioselective allylation step.[6a,b] Piplartine (**3**), used in the preliminary biological assays, was isolated from the roots of *Piper tuberculatum* and was kindly provided by Prof. Edilberto Rocha Silveira from the Federal University of Ceará, Brazil.[13] We then developed an alternative synthetic route. As outlined in Scheme 1, the synthesis started with the preparation of lactam **9** in a two-step sequence involving the formation of homoallyl crotonamide **8**, followed by ring-closing metathesis by using a Grubbs second-generation catalyst. Next, 3,4,5-trimethoxycinnamic acid (**12**), obtained from 3,4,5-

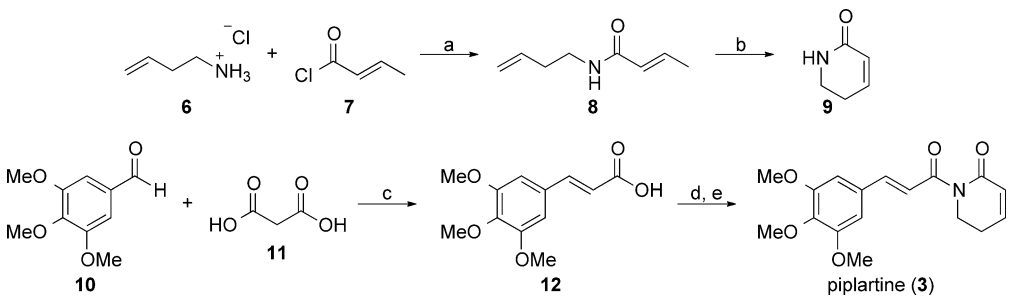

Scheme 1. Synthesis of piplartine (**3**). *Reagents and conditions:* a) Et_3N, DMAP (cat.), CH_2Cl_2, 0 °C→RT, 2 h, 79%; b) Grubbs 2nd-gen. catalyst (2.5 mol%), CH_2Cl_2, reflux, 2 h, 94%; c) piperidine (cat.), pyridine, 130 °C, 2 h, then 5% aq. HCl, 87%; d) oxalyl chloride, DMF (cat.), CH_2Cl_2, 0 °C→RT, 2 h; e) lactam **9**, Et_3N, DMAP (cat.), THF, RT, 40 h, 67% (over two steps). DMAP: 4-dimethylaminopyridine.

trimethoxybenzaldehyde (**10**) through a Knoevenagel–Dobner condensation by using modified reaction conditions,[14] was converted into the corresponding acid chloride by using oxalyl chloride and the acid chloride was combined with lactam **9** in the presence of triethylamine and catalytic *N*,*N*-dimethylaminopyridine to furnish piplartine (**3**) in good overall yield and with spectroscopic data identical to those described in the literature.[15]

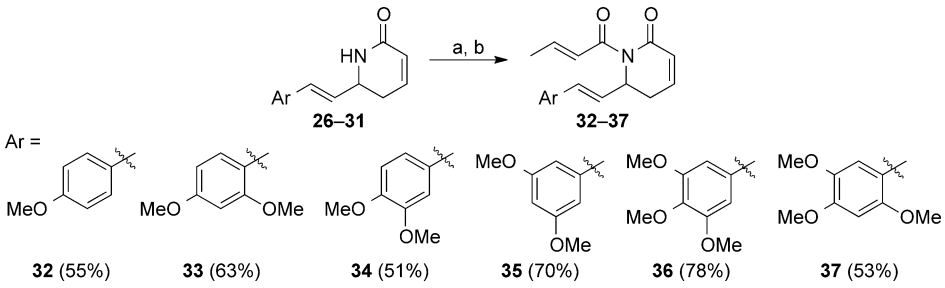

Scheme 3. Synthesis of N-acylated aza-goniothalamin derivatives **32**–**37**. *Reagents and conditions:* a) LHMDS (1.3 equiv), THF, −78 °C, 15 min; b) crotonyl chloride (2.0 equiv), THF, −78 °C→RT, 2 h.

The synthesis of racemic N-acylated aza-goniothalamin derivatives was accomplished by N-acylation of aza-goniothalamin (**2**), which was prepared on a gram scale by using the conditions described in our previous work.[7g] As depicted in Scheme 2, acylation of the lactam nitrogen atom of **2** was performed by deprotonation with LHMDS at −78 °C and subsequent treatment with a variety of acid chlorides or methyl chloroformate. Alternatively, the mixed anhydride was generated in situ after treatment of the carboxylic acid of interest with pivaloyl chloride. The N-acylated analogues **13**–**19** were obtained in good to excellent yields (53–98%). For phenolic derivatives, removal of the TBS protecting group was accomplished by using a solution of hydrogen fluoride pyridine complex (Scheme 2) and led to the formation of compounds **23**–**25**, which were obtained in good yields (up to 94%).

In addition to these compounds, we also prepared racemic polymethoxylated *N*-crotonyl aza-goniothalamin derivatives **32**–**37** (Scheme 3) by acylation of the aza-goniothalamin analogues **26**–**31**, prepared in our previous work.[7g] All compounds prepared were purified by flash column chromatography and characterized by FTIR spectroscopy, ^{1}H and ^{13}C NMR spectroscopy, and HRMS. The purity of the final compounds was verified by UPLC analysis. The NMR spectra of the compounds prepared are available in the Supporting Information.

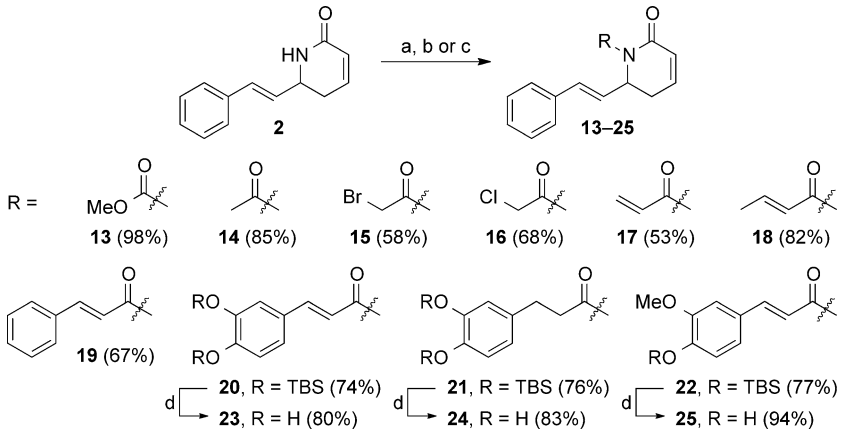

Scheme 2. Synthesis of N-acylated aza derivatives **13**–**25**. *Reagents and conditions:* a) LHMDS (1.3 equiv), THF, −78 °C, 15 min; b) RCOCl or $ClCO_2Me$ (2.0 equiv), THF, −78 °C→RT, 2 h (for compounds **13**–**16**, **18**, and **19**); c) RCO_2H (1.2 equiv), *t*BuCOCl (1.2 equiv), Et_3N (1.6 equiv), THF, 0 °C, 30 min, then the solution prepared in (a), 0 °C→RT, 2 h (for compounds **17** and **20**–**22**); d) HF·py, pyridine, THF, 0 °C, 2 h. LHMDS: lithium hexamethyldisilazanide, py: pyridine, TBS: *tert*-butyldimethylsilyl.

2.2. In vitro biological activities

2.2.1. Evaluation of in vitro antiproliferative activity against human cancer cells

The antiproliferative activity of all of the goniothalamin derivatives was evaluated in vitro against eight different human cancer cell lines: U251 (glioma), MCF-7 (breast), NCI-ADR/RES (ovarian expressing multiple-drug-resistance phenotype), 786-0 (kidney), NCI-H460 (lung non-small cells), PC-3 (prostate), OVCAR-3 (ovarian), and HT-29 (colon). To evaluate the potential selectivity for tumor cells, the cytotoxic activity of each compound was also evaluated in vitro against spontaneously transformed keratinocytes from histologically normal skin (HaCat cells). Doxorubicin was employed as the positive control. Goniothalamin (**1**) and piplartine (**3**) were included as reference compounds.

Cell proliferation was determined spectrophotometrically by using sulforhodamine B (SRB) as a protein-binding dye, and analyses were based on the US National Cancer Institute (NCI) 60 human tumor cell line anticancer drug screen (NCI60).[16] In this assay, measurement of the cell population density at time zero (the time at which the drugs are added) is possible, which allows the calculation of the cellular responses for total growth inhibition. The drug concentration resulting in total growth inhibition (TGI) is calculated from $T = T0$, in which the amount of protein at the end of drug incubation (T) is equal to the amount at the beginning ($T0$).[16a]

Goniothalamin (**1**), aza-goniothalamin (**2**), piplartine (**3**), derivatives **13**–**19**, **23**–**25**, and **32**–**37**, caffeic acid (**38**), and ferulic acid (**39**) were employed at concentrations of 0.25–250 μg mL^{-1},

whereas doxorubicin was evaluated at concentrations of 0.025–25 μg mL^{-1}. The TGI value was determined after 48 h of cell treatment. The initial in vitro screening was planned to select the best candidates for antitumor activity evaluation in animal models and, eventually, in clinical trials.

The evaluation of the antiproliferative activity of goniothalamin (**1**), aza-goniothalamin (**2**), piplartine (**3**), derivatives **13**–**19** and **23**–**25**, and cinnamic acids **38** and **39** is summarized in Table 1, which displays the TGI value for each compound.

In general, piplartine (**3**) was more potent than goniothalamin (**1**) against most of the tumor cell lines evaluated, and it was up to seven times less toxic to HaCat cells than to cancer cell lines. These results are consistent with a recent study performed by Raj et al. with a different panel of tumor cell lines, in which piplartine (**3**) was shown to selectively kill cancer cells with no toxicity to untransformed normal cells.[10b]

In a previous work from our group,[7g] we aimed at synthesizing goniothalamin derivatives with isosteric substitution of the lactone ring by the corresponding lactam core. A series of aza-goniothalamin analogues was prepared, and their evaluation against a series of tumor cell lines revealed that the introduction of the lactam ring completely abolished their in vitro antiproliferative activity. As can be seen in Table 1, aza-goniothalamin (**2**), a representative of this series, had no significant antiproliferative activity, even at the highest concentration tested (250 μg mL^{-1}).

SAR studies have indicated that the high cytotoxic activity presented by goniothalamin (**1**) and its congeners is related to the α,β-unsaturated δ-lactone scaffold, which could potentially act as a Michael acceptor in biological systems.[7f,8a,b,17] Michael acceptors can undergo heteroconjugate addition with nucleophilic thiols present in cysteine residues in irreversible[18] or reversible fashion.[19] In order to improve the electrophilic ability of the aza analogues of goniothalamin (**1**), a concise series of N-acylated aza derivatives was synthesized by acylation of the lactam nitrogen atom of aza-goniothalamin (**2**), which resulted in compounds **13**–**19** and **23**–**25** (Table 1).

As we anticipated, simple acylation and/or protection as a carbamate of the lactam nitrogen atom restored the activity of compounds **14** and **13** to the same level as that of goniothalamin (**1**). These compounds displayed moderate antiproliferative activity against kidney (786-0) and lung non-small tumor cells (NCI-H460), which confirmed the importance of the Michael acceptor core for the cytotoxic activity.

The introduction of an additional electrophilic site, such as in α-bromoacetyl derivative **15**, resulted in a compound that was threefold more potent than goniothalamin (**1**) against breast cancer cells (MCF7), yet seven times less toxic to HaCat cells than goniothalamin (**1**).

Additionally, *N*-acryloyl and *N*-crotonyl substitution resulted in derivatives **17** and **18** containing a second potentially electrophilic site that could influence their effect on cell viability. Interestingly, these analogues were more potent than the parent molecules, with low TGI values against most of the tumor cell lines evaluated. These derivatives exhibited promising antiproliferative activity against glioma (U251), breast (MCF-7), kidney (786-0), and prostate (PC-3) cancer cells and were even more potent than goniothalamin (**1**) and piplartine (**3**) in these cases. For example, derivative **18** showed TGI values as low as 3.9 and 7.2 μM for kidney (786-0) and prostate (PC-3) cancer cells, respectively, while this compound was approximately 38 times less toxic to HaCat cells when compared to kidney cancer cells. On the other hand, compounds **19**, **23** and **25** were less potent than derivatives **17** and **18** toward most of the cell lines evaluated. Their reduced cellular potency could probably be related to the higher steric hindrance caused by the aromatic ring of the cinnamoyl substitution.

In a recent work, Adams et al. synthesized and tested an array of piplartine analogues, and they have identified the *endo* double bond in the lactam ring as a key pharmacophore,

Table 1. TGI values for doxorubicin (DOX), goniothalamin (**1**), aza-goniothalamin (**2**), piplartine (**3**), compounds **13**–**19**, **23**–**25**, and cinnamic acids **38** and **39** toward various cell lines.

Compd	TGI [μM][a]								
	U251	MCF-7	NCI-ADR/RES	786-0	NCI-H460	PC-3	OVCAR-3	HT-29	HaCat
DOX	5.6 ± 0.0	1.2 ± 0.0	66.3 ± 5.9	9.0 ± 0.1	20.4 ± 0.4	0.8 ± 0.1	11.9 ± 0.1	61.7 ± 2.6	6.3 ± 0.6
1	24.7 ± 2.1	76.1 ± 2.3	72.5 ± 4.4	21.0 ± 2.9	22.6 ± 3.3	17.2 ± 0.8	20.2 ± 1.5	34.7 ± 4.8	49.0 ± 14.7
2	942.5 ± 11.4	> 1254	> 1254	> 1254	> 1254	> 1254	> 1254	> 1254	> 1254
3	18.6 ± 2.5	55.9 ± 0.5	22.8 ± 2.7	15.4 ± 1.1	31.4 ± 2.7	22.2 ± 2.6	25.5 ± 1.3	15.8 ± 1.9	120.2 ± 6.4
13	67.6 ± 2.3	113.6 ± 4.0	488.2 ± 11.3	64.1 ± 1.9	58.1 ± 0.2	148.5 ± 9.2	159.6 ± 3.6	285.4 ± 57.6	103.0 ± 3.2
14	48.8 ± 3.9	95.8 ± 6.6	288.9 ± 0.5	23.8 ± 4.9	32.3 ± 1.9	48.8 ± 2.8	50.3 ± 0.2	66.3 ± 8.1	110.2 ± 2.8
15	27.3 ± 1.5	26.6 ± 0.3	128.1 ± 23.7	16.2 ± 4.4	39.1 ± 0.2	20.7 ± 2.9	55.7 ± 10.8	87.6 ± 4.8	369.6 ± 1.7
16	25.7 ± 6.4	31.4 ± 2.9	78.3 ± 6.1	36.6 ± 1.0	43.0 ± 2.9	32.9 ± 5.9	46.6 ± 7.8	74.7 ± 2.6	97.8 ± 19.6
17	15.9 ± 0.5	11.3 ± 0.2	41.7 ± 7.0	6.2 ± 2.8	44.3 ± 4.7	17.4 ± 3.0	37.4 ± 8.4	47.6 ± 4.4	45.3 ± 2.6
18	10.9 ± 1.3	11.0 ± 0.9	61.8 ± 6.5	3.9 ± 0.5	25.1 ± 4.9	7.2 ± 2.3	15.5 ± 2.9	21.5 ± 0.7	150.2 ± 5.8
19	72.5 ± 2.2	44.1 ± 8.6	524.3 ± 18.1	41.1 ± 6.7	130.1 ± 7.4	53.4 ± 14.2	96.8 ± 13.1	183.2 ± 2.4	131.1 ± 1.5
23	35.9 ± 2.1	41.3 ± 4.7	37.3 ± 0.5	29.8 ± 4.6	37.1 ± 2.6	35.8 ± 7.5	58.0 ± 0.8	49.8 ± 0.6	40.8 ± 4.9
24	24.6 ± 3.3	26.6 ± 3.0	20.6 ± 0.6	36.5 ± 0.6	60.7 ± 3.8	36.9 ± 2.2	45.7 ± 2.0	44.9 ± 2.0	63.3 ± 0.1
25	88.1 ± 3.6	37.8 ± 4.9	869.7 ± 74.0	57.8 ± 5.6	100.9 ± 4.6	161.3 ± 12.3	222.7 ± 5.4	39.4 ± 4.2	300.8 ± 9.7
38	> 1388	> 1388	> 1388	> 1388	> 1388	> 1388	> 1388	> 1388	> 1388
39	> 1287	> 1287	> 1287	> 1287	> 1287	> 1287	> 1287	> 1287	> 1287

[a] The concentration that elicits total growth inhibition (TGI) was determined from nonlinear regression analysis by using ORIGIN 8.0 software (OriginLab Corporation). Results are expressed as the mean ± standard error of mean (SEM) from two different experiments in triplicate.

with the exocyclic double bond also playing a significant role in determining toxicity.[20] In a comparison of the activity of derivatives **23** and **24**, the *exo* double bond seems to be less important for the antiproliferative activity of this family of compounds against the panel of cancer cell lines used in our study, as both compounds exhibited the same level of activity in the assays. On the other hand, the selectivity presented by derivative **25** possessing a 4-hydroxy-3-methoxycinnamoyl substituent toward breast (MCF-7) and colon (HT-29) tumor cells, with considerably lower toxicity for HaCat cells, is noteworthy.

Literature precedents indicate that cinnamic acids present cytotoxic activity against different human cancer cell lines,[21] depending on the number of hydroxy groups in the aromatic ring and the degree of saturation of the carbon chain within the molecule. This is proposed to be due to a balance between the antioxidant and pro-oxidant properties of this family of compounds. Among the phenols described in the literature, caffeic acid (**38**) exhibited efficient antiproliferative activity against all the cell lines evaluated, particularly for cervical cancer cells (HeLa cells).[21a] Caffeic acid (**38**) was reported to inhibit angiogenesis, tumor invasion, and metastasis.[21c] More recently, it was found to inhibit tumor growth and angiogenesis by inhibiting the activity of the signal transducer and activator of transcription 3 (STAT3) and the expression of hypoxia inducible factor-1a (HIF-1a) and vascular endothelial growth factor (VEGF) in a mouse xenograft model.[22]

To evaluate whether the antiproliferative profiles observed for compounds **23** and **25** were due to the *N*-cinnamoyl substitution, phenolic acids **38** and **39** (caffeic and ferulic acids, respectively), which were used in the synthesis of these derivatives, were also evaluated against the same panel of human tumor cell lines. As shown in Table 1, these acids did not present significant antiproliferative activity against any of the cell lines evaluated, even at the higher concentration used in the SRB cytotoxicity assay (TGI values greater than 250 $\mu g\,mL^{-1}$).

In our previous work, a series of polymethoxylated goniothalamin analogues was prepared to afford compounds more potent than goniothalamin (**1**) toward the panel of cancer cell lines.[7g] N-Acylation of the nitrogen atom of aza-goniothalamin (**2**) significantly enhanced the antiproliferative activity, so we decided to prepare a new series of N-acylated aza-goniothalamin derivatives possessing different degrees of methoxylation in the styryl side chain. In view of the higher activity of derivative **18**, crotonyl chloride was selected for the acylation of the aza-goniothalamin series (compounds **26**–**31**), to afford derivatives **32**–**37**.

The antiproliferative activity of compounds **32**–**37** was assessed against the same panel of eight human tumor cell lines by using the SRB cytotoxicity assay, with goniothalamin (**1**), piplartine (**3**), and derivative **18** as reference compounds. The results are summarized in Table 2, which displays the TGI value for each compound.

In general, the presence of methoxy groups at specific positions in the aromatic ring led to more potent analogues than derivative **18**, goniothalamin (**1**), or piplartine (**3**). For example, derivative **33** displaying 2,4-dimethoxy substituents was highly cytotoxic, with low TGI values particularly against breast (MCF-7), kidney (786-0), ovarian (OVCAR-3), and colon (HT-29) cancer cells. This compound also displayed higher potency than doxorubicin against ovarian expressing multiple-drug-resistance phenotype (NCI-ADR/RES), kidney (786-0), ovarian (OVCAR-3), and colon (HT-29) cancer cells. Interestingly, the same substitution pattern (2,4-dimethoxy) afforded the most active compound in the polymethoxylated goniothalamin series in our previous work.[7g] One could speculate that these methoxy groups could have a privileged interaction with putative hydrogen-bonding donors at the binding site of the biological target.

3,5-Dimethoxy substitution was also very effective (compound **35**) and resulted in improved antiproliferative activities against breast (MCF-7), ovarian expressing multiple-drug-resistance phenotype (NCI-ADR/RES), lung (NCI-H460), prostate (PC-3), ovarian (OVCAR-3), colon (HT-29), and particularly, kidney cancer cells (786-0). However, despite their potent antiproliferative activities against tumor cells, compounds **33** and **35** were more toxic to HaCat cells than derivative **18** and goniothalamin (**1**). 3,4,5-Trimethoxy-substituted analogue **36** exhibited similar antiproliferative activity against ovarian expressing multiple-drug-resistance phenotype (NCI-ADR/RES), lung non-small cells (NCI-H460, ovarian (OVCAR-3) and colon (HT-29) cancer cells to that of derivative **18**, but was less toxic to HaCat cells than compounds **33** and **35**.

Table 2. TGI values for doxorubicin (DOX), goniothalamin (**1**), piplartine (**3**), and compounds **18** and **32**–**37** toward various cell lines.

Compd	TGI [μM][a]								
	U251	MCF-7	NCI-ADR/RES	786-0	NCI-H460	PC-3	OVCAR-3	HT-29	HaCat
DOX	5.6 ± 0.1	1.2 ± 0.1	66.3 ± 5.9	9.0 ± 0.1	20.4 ± 0.4	0.9 ± 0.1	11.9 ± 0.1	61.7 ± 2.6	6.3 ± 0.6
1	24.7 ± 2.1	76.1 ± 2.3	72.5 ± 4.4	21.0 ± 2.9	22.6 ± 3.3	17.2 ± 0.8	20.2 ± 1.5	34.7 ± 4.8	49.0 ± 14.7
3	18.6 ± 2.5	55.9 ± 0.5	22.8 ± 2.7	15.4 ± 1.1	31.4 ± 2.7	22.2 ± 2.6	25.5 ± 1.3	15.8 ± 1.9	120.2 ± 6.4
18	10.9 ± 1.3	11.0 ± 0.9	61.8 ± 6.5	3.9 ± 0.5	25.1 ± 4.9	7.2 ± 2.3	15.5 ± 2.9	21.5 ± 0.7	150.2 ± 5.8
32	170.5 ± 15.7	28.6 ± 11.0	664.8 ± 41.3	25.0 ± 2.2	88.5 ± 19.5	33.9 ± 5.6	102.3 ± 29.6	70.4 ± 17.4	183.1 ± 1.2
33	30.2 ± 5.5	7.3 ± 1.0	19.1 ± 1.1	6.8 ± 1.2	41.8 ± 6.2	13.4 ± 1.3	7.9 ± 2.0	7.0 ± 0.2	23.5 ± 6.1
34	58.0 ± 4.8	19.8 ± 0.4	318.0 ± 1.7	16.2 ± 3.0	49.9 ± 4.2	17.2 ± 0.5	27.3 ± 0.6	17.4 ± 4.0	37.4 ± 0.3
35	48.3 ± 12.0	5.8 ± 1.9	35.9 ± 1.6	5.3 ± 2.0	19.2 ± 8.0	6.8 ± 3.8	12.3 ± 3.3	12.3 ± 4.1	27.6 ± 5.6
36	38.7 ± 3.9	28.5 ± 0.8	56.6 ± 1.4	14.6 ± 1.3	31.8 ± 4.3	22.0 ± 3.8	15.8 ± 1.1	14.8 ± 2.0	88.0 ± 13.7
37	113.3 ± 0.6	30.0 ± 0.3	135.0 ± 1.8	223.3 ± 3.6	65.2 ± 1.0	71.9 ± 3.1	37.8 ± 0.5	30.4 ± 3.0	88.0 ± 13.6

[a] The concentration that elicits total growth inhibition (TGI) was determined from nonlinear regression analysis by using ORIGIN 8.0 software (OriginLab Corporation). Results are expressed as the mean ± SEM from two different experiments in triplicate.

2.2.2. Goniothalamin (1) and derivative 18 induce apoptosis in PC-3 cells

In view of the higher cytotoxicity of derivative **18** against most of the human tumor cell lines evaluated and PC-3 being one of the most sensitive cell line towards derivative **18,** it was selected for further mechanistic evaluations.

Prostate cancer is the most common type of cancer in men and its incidence is increasing year after year. In the USA, 233 000 new cases of prostate cancer are expected in 2014, with 29 480 deaths.[1] Well-established risk factors for prostate cancer include aging, African ancestry, and a family history of prostate cancer. Among the human prostate tumor cell lines, PC-3 is very aggressive and represents hormone-insensitive prostate cancer, which currently remains untreatable.[23]

The exposure of phosphatidylserine (PS) on the surface of apoptotic cells is one of the best-characterized surface changes that facilitate recognition and engulfment of dying cells, because plasma membranes of viable cells exhibit substantial phospholipid asymmetry, with most of the PS residing on the inner leaflet of the plasma membrane.[24] One of the methods used for the assessment of apoptosis is the double staining for Annexin V and 7-amino-actinomycin D (7-AAD) by flow cytometry analysis. Annexin V is a protein with high affinity for PS and binds to PS translocated to the outer face of the cell membrane during the initial process of apoptosis (early apoptosis). 7-AAD binds to the DNA of the cell and acts as an indicator of membrane structural integrity, because it is not able to enter viable cells and early apoptotic cells; thus, it indicates late apoptosis. For apoptosis evaluation, we performed the Annexin V/7-AAD double-staining assay by flow cytometry.

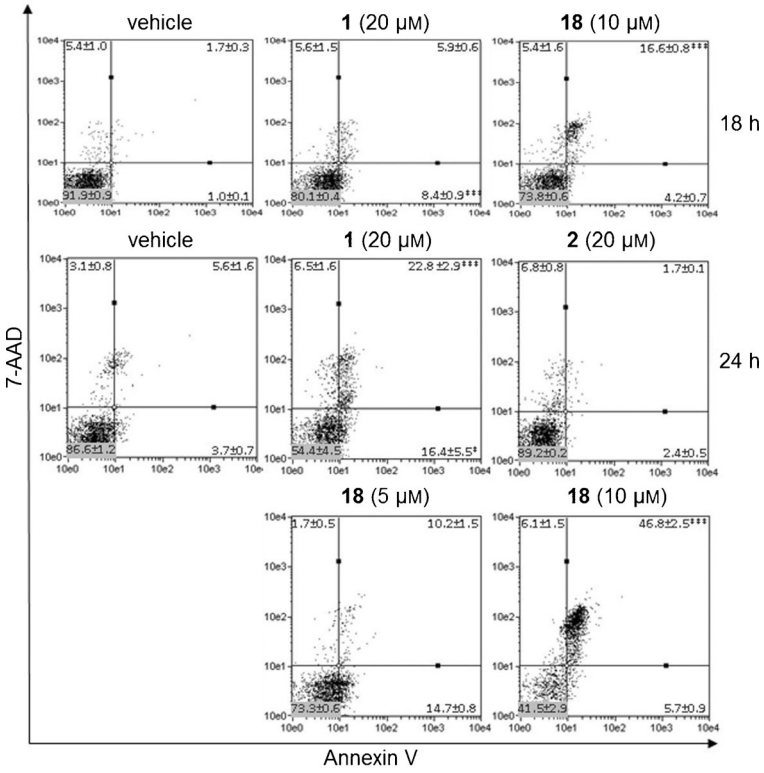

Figure 2. Goniothalamin (**1**, 20 μM) and derivative **18** (10 μM) induce apoptosis in PC-3 cells after 18 h of treatment. Aza-goniothalamin (**2**) and derivative **18** at concentrations of 20 and 5 μM, respectively, were not able to induce apoptosis during the experiment. Cells were exposed to vehicle (DMSO), goniothalamin (**1**), aza-goniothalamin (**2**), and derivative **18** for 18 and 24 h at the concentrations shown above and analyzed by flow cytometry by using the Annexin V/7-AAD double-staining assay. Representative dot plots from three different experiments conducted in triplicate are shown. Values in each quadrant are the mean ± SE, in percentage of cells; ***$p < 0.001$, statistical analysis by Tukey's multiple comparison test and analysis of variance (ANOVA), statistically different from the vehicle results.

As discussed previously, after 48 h of treatment, goniothalamin (**1**) and derivative **18** elicited total growth inhibition in PC-3 cells, with TGI values of (17.2 ± 0.8) and (7.2 ± 2.3) μM, respectively (Table 1). In order to evaluate apoptosis induction, cells were treated with goniothalamin (**1**; 20 μM concentration) and derivative **18** (5 and 10 μM concentration) and assayed after 6, 15, 18, and 24 h of treatment. For the sake of comparison, aza-goniothalamin (**2**) was employed at 20 μM concentration.

Treatment with derivative **18** at 5 μM concentration was not able to induce apoptosis, even after 24 h (Figure 2). However, at a higher concentration (10 μM), it induced PS externalization after 18 h, at which time (16.6 ± 0.8) % of the cells were double stained with Annexin V and 7-AAD, which indicated late apoptosis. After 24 h, the amount of late apoptotic cells increased to (46.8 ± 2.5) %. Similarly, treatment with goniothalamin (**1**), at a concentration of 20 μM, induced PS externalization after 18 h, at which time (5.9 ± 0.6) % of the cells were in late apoptosis. After 24 h of treatment, the incidence had increased to (22.8 ± 2.9) %. As might be expected, treatment with aza-goniothalamin (**2**), at a concentration of 20 μM, was not able to induce apoptosis (Figure 2). The data for 6 and 15 h are not shown because of the absence of apoptotic cells.

These results are in agreement with the antiproliferative activity assay on the panel of tumor cell lines, in which both compounds **1** and **18** are capable of eliciting total growth inhibition and cell death. In those experiments, derivative **18** was more potent than goniothalamin (**1**), as can be observed in the flow cytometry analyses above. Similar to the antiproliferative activity assay, compound **2** did not induce cell death.

As we observed apoptosis induction by compounds **1** and **18**, we next investigated the induction of caspase activation following exposure to these compounds. Cells were analyzed after 18 and 24 h of treatment, because PS externalization was evident at these times. Thus, treatment with goniothalamin (**1**; 20 μM) and derivative **18** (10 μM) induced significant caspase activation after 18 h of treatment in (21.5 ± 1.3) % and (34.3 ± 1.7) % of the cells, respectively (Figure 3). After 24 h of treatment, this effect was more pronounced and caspase activation occurred in (43.5 ± 2.3) % and (77.2 ± 5.0) % of the cells treated with goniothalamin (**1**) and derivative **18**, respectively (Figure 3).

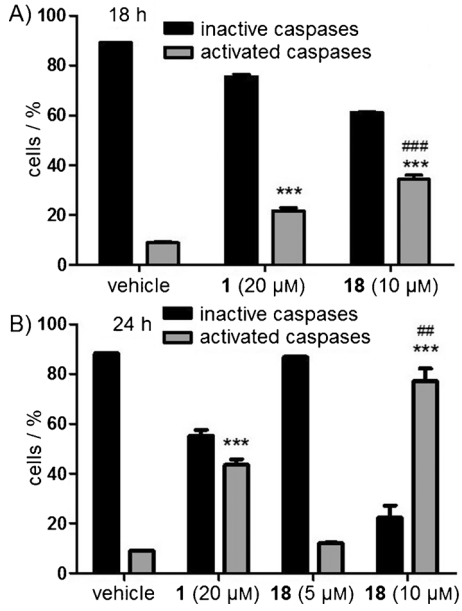

Figure 3. Multicaspase activation in PC-3 cells after treatment with goniothalamin (**1**, 20 μM) and derivative **18** (10 μM) for A) 18 and B) 24 h. According to the Annexin V results, treatment with goniothalamin (**1**, 20 μM) and derivative **18** (10 μM) activates caspases after 18 h of treatment. Results are represented by the mean ± SE, in percentage of cells; $^{\#\#}p < 0.01$, $^{\#\#\#***}p < 0.001$; statistical analysis by Tukey's multiple comparison test and ANOVA. *: Statistically different from vehicle results; #: statistically different from goniothalamin (**1**).

Taken together, these results point to a similar activity profile conferred by goniothalamin (**1**) and derivative **18** in PC-3 cells: caspase-dependent apoptosis after 18 h of treatment. However, derivative **18** is more potent than goniothalamin (**1**), because treatment with **18** (10 μM) led to a higher percentage of cells in apoptosis than treatment with goniothalamin (**1**) at a higher concentration (20 μM).

Three main types of biochemical changes can be observed in apoptosis: 1) activation of caspases, 2) DNA and protein breakdown leading to membrane changes, and 3) recognition by phagocytic cells (for example, by PS externalization).[25] As shown earlier, we observed that both caspase activation and PS externalization were induced by goniothalamin (**1**) and derivative **18**. In addition to these biochemical changes, we also observed morphological evidence of cell death, for example, cell detachment and loss of typical morphology after treatment with these compounds (Figure 4). As expected, treatment with aza-goniothalamin (**2**) did not affect the cell morphology.

2.2.3. Derivative 18 induces G_2/M cell-cycle arrest in PC-3 cells

In apoptosis, caspases are both initiators and effectors. Downstream caspases (effectors) induce cleavage of protein kinases, cytoskeletal proteins, DNA repair proteins, and inhibitory subunits of endonucleases family and, thus, affect cell cycle and signaling pathways, which together contribute to the typical morphological changes in apoptosis.[25] The complex network of apoptosis and cell cycle are closely linked. Many of the cancer cell treatments with anticancer agents usually result in cell-cycle arrest, which subsequently leads the cells to enter apoptosis.[26]

To evaluate possible interference of goniothalamin (**1**) and derivative **18** in the PC-3 cell cycle, we performed cell-cycle analysis by flow cytometry. For this study, cells were treated with non-apoptotic concentrations of goniothalamin (**1**) and derivative **18** for 24 h, because concentrations that elicit apoptosis would promote a sub-G_1 phase arrest. The cell-cycle distribution of treated PC-3 cells is presented in Figure 5.

As can be seen, treatment with a 5 μM concentration of derivative **18** resulted in arrest of the G_2/M phase in (48.9 ± 2.3) % of the cells. On the other hand, treatment with goniothalamin (**1**) at a concentration of 10 μM did not interfere with cell cycle, although there was an increase in the percentage of cells in the sub-G_1 phase to (11.3 ± 0.9) %, which could indicate DNA fragmentation and apoptosis. As expected, colchicine (1.25 nM) increased the percentage of cells in the G_2/M phase (up to (71.4 ± 4.2) %), which was accompanied by a decreased percentage of cells in the G_1 phase. No interference on the cell-cycle profile was observed with aza-goniothalamin (**2**) at a concentration of 20 μM.

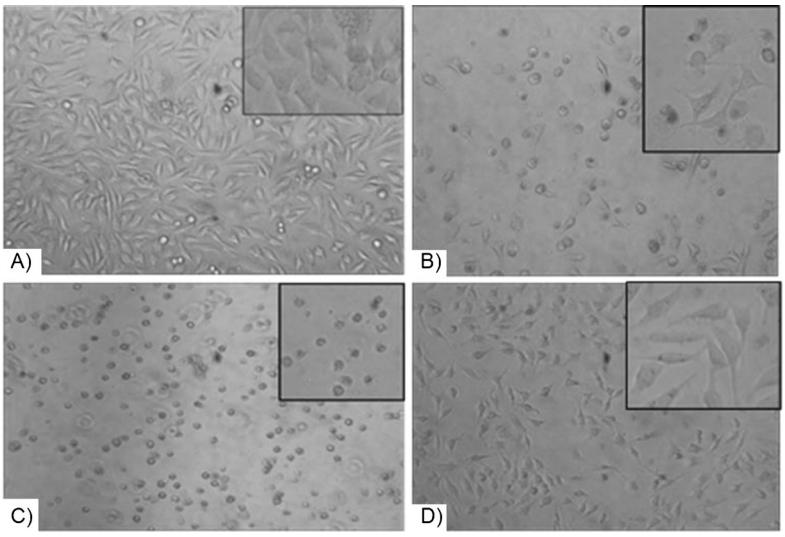

Figure 4. Cell morphology after 24 h treatment with: A) vehicle (DMSO), B) goniothalamin (**1**, 20 μM), C) derivative **18** (10 μM), and D) aza-goniothalamin (**2**, 20 μM). In A and D, the PC-3 morphology is maintained and cells are attached. In B and C, there is a loss of typical morphology and cell detachment, which is a feature of cell death. Photomicrographs were taken with an Optikam B3 digital camera on a Leica DM IL inverted microscope with a 10×/0.25 objective (details with a 20×/0.3 objective).

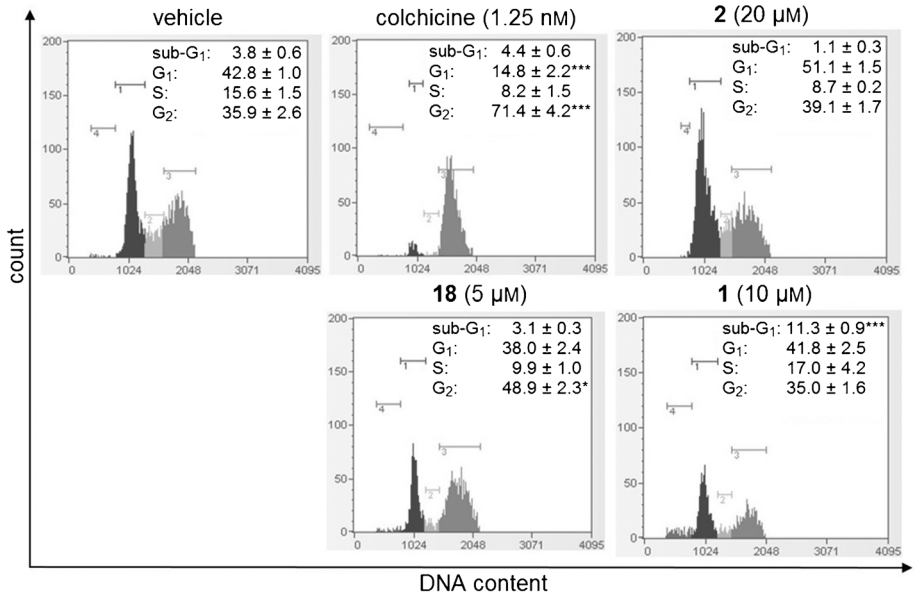

Figure 5. Cell-cycle effects of vehicle (DMSO), colchicine (1.25 nM), aza-goniothalamin (**2**, 20 μM), derivative **18** (5 μM), and goniothalamin (**1**, 10 μM) on PC-3 cells after 24 h of treatment. Flow cytometry analyses of DNA content shows that derivative **18** arrests PC-3 cells in the G_2/M phase, like the positive control colchicine. Goniothalamin (**1**) promotes sub-G_1 arrest, which indicates apoptosis (DNA fragmentation). Neither aza-goniothalamin (**2**) nor the vehicle affect the PC-3 cell cycle. In the graph, the gated sections represent the phases 1: G_1, 2: S, 3: G_2/M, and 4: sub-G_1. Representative histograms from three different experiments conducted in triplicate are shown. The results are represented by the mean ± SE, in percentage of cells; $*p < 0.05$, $***p < 0.001$; statistical analysis by Tukey's multiple comparison test and ANOVA.

In contrast to derivative **18**, goniothalamin (**1**) did not induce changes in the PC-3 cell-cycle profile, which indicates a different mechanism of action for the two compounds: derivative **18** might regulate PC-3 proliferation by inhibiting cell-cycle progression through the G_2/M phase. Progression through each phase of the cell cycle is monitored by checkpoints that detect aberrant or incomplete events and signal cell-cycle arrest until the problem is solved.[27] The G_2/M checkpoint ensures that cells do not initiate mitosis before problems occurred during replication in the S phase are repaired. The G_2/M cell-cycle arrest induced by derivative **18** could be a response to DNA damage or events during mitosis, such as tubulin stabilization. Further studies should be conducted to confirm this hypothesis.

2.2.4. Goniothalamin (1) and derivative 18 induce intracellular ROS generation

In cancer, there is an imbalance between cell division and cell death.[25] Evasion of cell death signals is one of the hallmarks of tumor cells that favors their maintenance, which has thus stimulated an active search for anticancer regimens that induce apoptosis.[28] Several small molecules, such as phenethylisothiocyanate (PEITC),[29a] parthenolide,[29b] piplartine (**3**),[10b] erastin,[29c] lanperisone,[29d] and molecules containing disulfide, α,β-unsaturated carbonyl, sulfonate, or other electrophilic functional groups, have been shown to induce cancer cell death by intracellular ROS generation through conjugation with glutathione (GSH), causing its depletion, or targeting its synthesis.[20,30] As both goniothalamin (**1**) and derivative **18** possess α,β-unsaturated carbonyl systems, we evaluated intracellular ROS generation.

ROS function as signaling molecules produced by normal cells during normal metabolic activities and are cleared by endogenous antioxidant systems. The balance between ROS generation and its depletion is an essential event in living organisms.[31] Oxidative stress occurs when this balance is disturbed due to a high level of ROS production and a reduced level of ROS-scavenging systems. ROS and cellular oxidative stress have long been associated with cancer, both in culture and in vivo, relative to normal cells.[30,32]

To evaluate intracellular ROS generation, a 2′,7′-dichlorodihydrofluorescein diacetate (DCFH-DA) probe was employed. It readily diffuses into the cells and is hydrolyzed to the polar derivative 2′,7′-dichlorodihydrofluorescein (DCFH), with the latter being oxidized in the presence of hydrogen peroxide generated by ROS to the highly fluorescent 2′,7′-dichlorofluorescein (DCF). After one hour of treatment, intracellular ROS levels increased tenfold in cells treated with a 20 μM concentration of goniothalamin (**1**), in comparison with those with the control, whereas an increase of approximately sixfold was observed in cells treated with a 10 μM concentration of derivative **18** (Figure 6). Treatment with derivative **18** at a lower concentration (5 μM) or aza-goniothalamin (**2**; 20 μM) did not induce significant ROS generation. These results are in agreement with the apoptotic assays, because 5 μM concentrations of derivative **18** or aza-goniothalamin (**2**) were not able to induce apoptosis. Otherwise, derivative **18** (at 10 μM) and goniothalamin (**1**; at 20 μM) induced intracellular ROS generation, which thus links oxidative stress to cell death.

The pro-apoptotic activity and induction of ROS generation in PC-3 cells promoted by goniothalamin (**1**) and derivative **18** are in agreement with the literature data. There are several reports of goniothalamin (**1**) having pro-apoptotic activity in different tumor cell lines: PS exposure and caspase activation were observed in Jurkat and HL-60 leukemic cell lines after treatment with 50 μM goniothalamin (**1**) after 5 and 14 h, respectively.[7a,b] Goniothalamin (**1**) also induced apoptosis in vascular smooth muscle (VSM) cells with DNA damage, after 2 h of treatment.[33] Treatment with a 30 μM concentration of goniothalamin (**1**) induced apoptosis, ROS generation, and G_2/M cell-cycle arrest in MDA-MB-231 breast adenocarcinoma.[34] Furthermore, treatment of Jurkat and oral squamous cancer (Ca9-

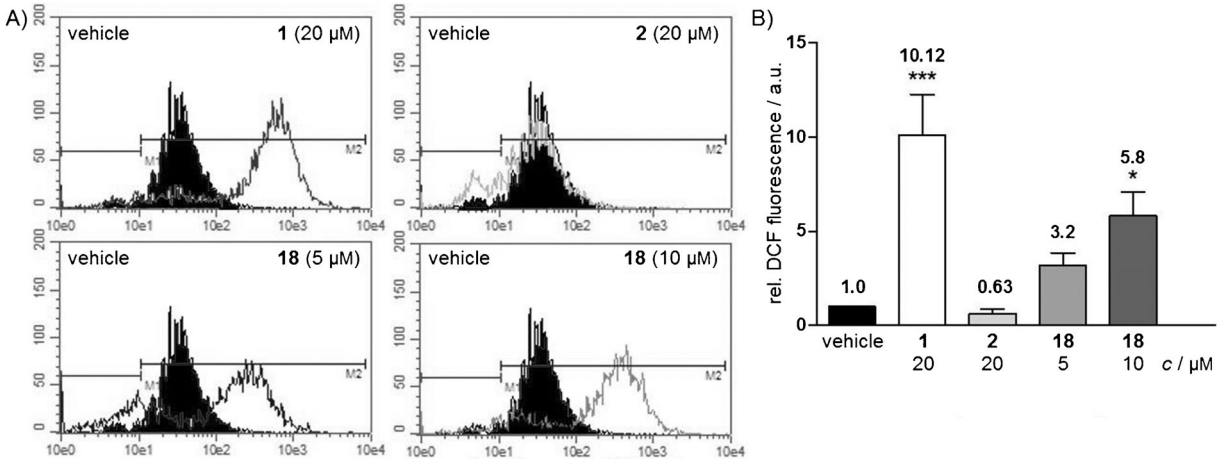

Figure 6. A) Relative DCF fluorescence in PC-3 cells after treatments with vehicle (DMSO, black fill), aza-goniothalamin (**2**, 20 μM), derivative **18** (5 and 10 μM), and goniothalamin (**1**, 20 μM) for 1 h. Flow cytometric analysis of DCF fluorescence shows that goniothalamin (**1**) and derivative **18** (10 μM) promote an increase in fluorescence by 10.12- and 5.8-fold, respectively, which is directly related to ROS generation. Neither aza-goniothalamin (**2**), derivative **18** (5 μM), nor the vehicle promoted ROS generation. B) Representative histograms from three different experiments conducted in triplicate are shown. The results are represented by relative fluorescence, in arbitrary units, normalized with the vehicle; $*p < 0.05$, $***p < 0.001$; statistical analysis by Tukey's multiple comparison test and ANOVA.

22) cells with goniothalamin (**1**) led to ROS generation, GSH depletion, DNA damage, and apoptosis.[35]

The relationship between ROS and cancer is complex and often paradoxical: 1) ROS generation and oxidative stress can induce cancer; 2) transformed cells produce more ROS than normal cells; 3) antioxidant systems are increased in malignant cells; 4) increased oxidative stress has a pivotal role in the development and progression of cancer by immortalization and transformation, cell proliferation and mitogenic signaling, cell survival and disruption of cell death signaling and metastasis; and 5) various chemotherapeutic agents are selectively toxic to tumor cells by inducing oxidative stress.[30,32]

The ROS generation promoted by goniothalamin (**1**) and derivative **18** could be, in part, explained by their capacity to interact with GSH through conjugate addition. In the same line of reasoning, the maintenance of basal levels of ROS when the cells were treated with aza-goniothalamin (**2**) could also be explained by the nonaddition of GSH to the α,β-unsaturated system of aza-goniothalamin (**2**).

2.2.5. Evaluation of the chemical reactivity of goniothalamin (1), aza-goniothalamin (2), piplartine (3), and N*-acyl-aza--goniothalamin derivatives in the presence of glutathione*

GSH is a natural pseudotripeptide, consisting of glutamate, cysteine, and glycine, found within almost all cells, and essential for several vital cellular processes, including antioxidation, regulation of the redox environment, modulation of the immune response, and detoxification of xenobiotics in eukaryotic cells.[36] GSH is also known to be highly reactive and is often found conjugated to other molecules through its sulfhydryl moiety. GSH is the major endogenous antioxidant produced by cells and helps to protect cells from ROS generation. It is well established that ROS and electrophilic chemicals can damage DNA and that GSH can protect against this type of damage.[37] In order to experimentally probe the assumptions above for ROS generation, the chemical reactivity of aza-goniothalamin (**2**), piplartine (**3**), and N-acylated aza-goniothalamin derivatives in the presence of GSH was assessed.

With this in mind, a qualitative evaluation of the chemical reactivity was performed by using NMR spectroscopy: goniothalamin (**1**), aza-goniothalamin (**2**), piplartine (**3**), and *N*-crotonyl aza-goniothalamin derivative **18** at a concentration of 25 mM in dimethyl sulfoxide (DMSO) were treated with five equivalents of GSH at room temperature and analyzed by ^{1}H NMR spectroscopy over 24 h (Figure 7). As expected, the conjugate addition of GSH to goniothalamin (**1**) was almost complete after 24 h, as indicated by the disappearance of the C2–C3 double bond signals in the ^{1}H NMR spectrum (Figure 7 A). The same result was observed for piplartine (**3**), although the addition of GSH to the *endo* double bond occurred much faster than for goniothalamin (**1**; in approximately 7 h; Figure 7 B). Despite the fact that piplartine (**3**) contains two potentially electrophilic sites, treatment with five equivalents of GSH provided mainly the product of conjugate addition at the C3 position. This result is consistent with a recent study performed by Adams et al., who showed that addition of methyl thioglycolate to piplartine (**3**) takes place only at the C3 position.[38] On the other hand, no GSH addition was observed at the C3 position of the lactam ring of aza-goniothalamin (**2**) under the same conditions (Figure 7 C).

Surprisingly, when derivative **18** was treated with GSH, we observed not only addition at the C3 position of the lactam ring but also the disappearance of the C8–C9 double bond signals in the ^{1}H NMR spectrum (Figure 7 D), which thus indicated a higher electrophilicity of the crotonyl side chain relative to that of piplartine (**3**). Taken together, our findings corroborate the higher activity of the *N*-crotonyl aza-goniothalamin derivative **18** in comparison with those of goniothalamin (**1**) and piplartine (**3**), as a consequence of its double Michael

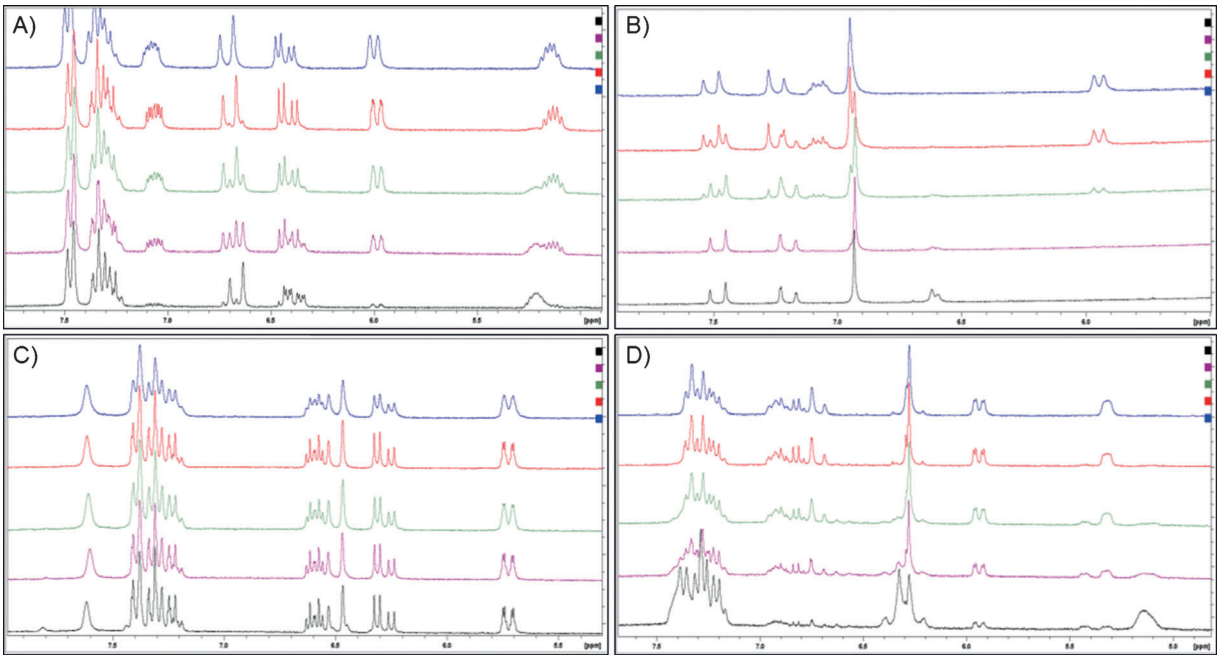

Figure 7. ^{1}H NMR spectra (250 MHz, [D_6]DMSO) obtained during the reaction of A) goniothalamin (**1**), B) piplartine (**3**), C) aza-goniothalamin (**2**), and D) derivative **18** with GSH (5 equiv) after addition (blue), 1 h (red), 3 h (green), 7 h (pink), and 24 h (black).

acceptor ability in the biological system, most likely due to stereoelectronic factors.

In agreement with our NMR study, compounds containing α,β-unsaturated lactone moieties have been reported to directly conjugate with GSH.[39a–e] GSH addition was found to deactivate these lactones, as shown by the decrease of cytotoxicity of sesquiterpene lactones in the presence of GSH.[39c] The expressive in vitro activity displayed by derivative **18** could, in principle, be rationalized by the model for the chemical-mediated protein glutathionylation of GSH-binding proteins proposed by Adams et al.[38] Accordingly, derivative **18** may react with GSH at its more electrophilic *endo* α,β-unsaturated system and the resulting adduct could interact with a GSH-binding protein. The formation of this noncovalent complex could finally trigger Michael addition of a nucleophilic residue of the GSH-binding protein to the less electrophilic *exo* α,β-unsaturated system, which would lead to the toxic effects observed in cells (that is, cell death). However, this model does not explain the good in vitro antiproliferative activity displayed by derivative **24**, which lacks the *exo* double bond, toward the panel of cancer cell lines evaluated in this study. Although it was not observed during our NMR experiments, we cannot exclude adduction of GSH or other thiol nucleophiles to the carbonyl group, which is expected to be much slower than the addition to the α,β-unsaturated system in piplartine (**3**) and derivative **18**.[40a,b]

ROS generation and the altered GSH redox state are linked with apoptotic signaling. Altered levels of ROS can down-regulate the anti-apoptotic FLICE inhibitory protein (FLIP-L) through c-Jun N-terminal kinase (JNK) activation, which can activate effector caspases. Moreover, ROS may lead to DNA damage, which activates the p53 pathway and results in cell-cycle arrest and apoptosis.[41] ROS generation is also associated with both intrinsic and extrinsic apoptotic pathways through mitochondrial outer membrane permeabilization and cytochrome *c* translocation to the cytosol. Activation of tumor necrosis factor receptor-1 (TNFR1) can also occur, which mediates apoptosis through clustering of receptors, signaling by lipid raft platforms, and interaction with nitric oxide (NO).[42] In all of those cases, caspases can be activated and lead to caspase-dependent apoptosis, as we observed for goniothalamin (**1**) and derivative **18**.

Our findings indicate that goniothalamin (**1**) and its most potent derivative **18** lead to ROS generation in PC-3 cells, which probably signals for caspase-dependent apoptosis. Both molecules interact with GSH and, thereby, stabilize the intrinsic mechanisms of ROS scavenging. Derivative **18** also leads to G_2/M cell-cycle arrest, which can be directly related to cell death or represents an additional antiproliferative mechanism.

2.3. In vivo studies

In view of the good in vitro antiproliferative activity displayed by derivative **18**, its in vivo antitumor activity was also evaluated in experimental models of Ehrlich ascitic and solid tumors in mice, in comparison with goniothalamin (**1**) and aza-goniothalamin (**2**). Previously, the in vivo antitumor activity of goniothalamin (**1**) was evaluated by our group, which revealed that goniothalamin (**1**) inhibits Ehrlich solid tumor development without signs of toxicity.[6e] Although aza-goniothalamin (**2**) did not present in vitro antiproliferative activity, being only cytostatic in these assays, we decided to evaluate its in vivo profile, because in vitro results may not necessarily reflect the in vivo effect due to the intervention of biotransformations, which

may account for the formation of cytotoxic metabolites in preparation for bioconjugation and excretion.

The Ehrlich tumor is a murine breast adenocarcinoma, which is an aggressive and fast growing carcinoma that is able to develop in both the ascitic or solid forms, depending on whether inoculation is administered intraperitoneally or subcutaneously, respectively. These cells generate a local inflammatory response characterized by increased vascular permeability, which accounts for edema formation, cell migration, and recruitment of the immune response.[43] The advantage of performing experiments with both the ascitic and solid forms is that, in the ascitic model, treatments were conducted in the site of tumor cell implantation (local action), whereas in the solid model, treatments were performed i.p. and cell implantation was in the subcutaneous (systemic action). Thus, evaluation of derivative **18** and aza-goniothalamin (**2**) in this model could bring information about their systemic profiles.

2.3.1. Acute toxicity

In order to establish the appropriate dose for the evaluation of the in vivo antitumor activity in mice, the acute toxicity was assessed after intraperitoneal (i.p.) administration of aza-goniothalamin (**2**) and derivative **18**. No evidence of acute toxicity could be observed during the first 4 h after i.p. administration of 50 and 100 mg kg^{-1} of each compound, respectively, nor during the following 15 days when the animals were kept under observation. Acute administration of derivative **18** at a dose of 150 mg kg^{-1} promoted convulsion and decreased locomotion, but no deaths were observed during the 15 days of observation. Thus, the dose selected for all compounds was 50 mg kg^{-1} in the Ehrlich ascitic tumor model, and doses were 30 mg kg^{-1} of goniothalamin (**1**) and aza-goniothalamin (**2**) and 40 mg kg^{-1} of derivative **18** for the solid model. As a positive control, the chemotherapeutic 5-fluorouracil (5-FU) was administered at 10 mg kg^{-1} day^{-1} by i.p. injection.

2.3.2. Goniothalamin (1) and aza-goniothalamin (2) inhibit in vivo tumor growth

In the ascitic model, after seven days of daily treatment, goniothalamin (**1**; 50 mg kg^{-1}, i.p.) inhibited Ehrlich ascitic tumor cell proliferation by 83.8%. A comparable inhibition value was obtained for the chemotherapeutic 5-FU (10 mg kg^{-1}, i.p.), which inhibited Ehrlich ascitic tumor growth by 83.7%. Surprisingly and contrary to the in vitro profile, treatment with aza-goniothalamin (**2**; 50 mg kg^{-1} i.p.) was able to inhibit tumor cell proliferation by 77.7%, whereas treatment with derivative **18** (50 mg kg^{-1}, i.p.) inhibited proliferation by only 42.9% (Figure 8A).

In view of its remarkable in vivo antitumor activity, one could suggest that aza-goniothalamin (**2**) might be metabolized or undergo conjugation at the lactam nitrogen atom, which would change the electronic profile of the α,β-unsaturated system and favor the antitumor activity. Conversely, derivative **18** exhibited an unexpected lower in vivo antitumor activity, even though the treatments were conducted at the same site of inoculation (intraperitoneally), which should facilitate the action of the compound.

To evaluate the systemic activity of the compounds, we performed the Ehrlich solid tumor model, in which cells were inoculated subcutaneously and treatments were conducted in the peritoneum. In this model, the treatment period was longer (15 days), and in view of the results obtained in the ascitic model, the selected doses were 30 mg kg^{-1} for compounds **1** and **2** and 40 mg kg^{-1} for compound **18** for the solid model. Treatments were conducted daily for 15 days, by the intraperitoneal route.

In agreement with the results obtained in the Ehrlich ascitic tumor model, treatment with goniothalamin (**1**), aza-goniothalamin (**2**), and 5-FU inhibited tumor growth by 58.6, 44.9, and 57.2%, respectively, with statistical difference relative to the negative control (vehicle) but no statistical difference between them (Figure 8B). Treatment with derivative **18** (40 mg kg^{-1}) failed to inhibit tumor growth, with only 11.9% of inhibition, which confirmed its loss of activity in the in vivo models (Figure 8B). This loss of activity is not unprecedented in anticancer research, because the antiproliferative activity in in vivo models may not necessarily reflect the in vitro activity due to the complex relationship between a tumor and its microenvironment.[44] Moreover, solid tumors are heterogeneous and complex structures: within these tumors are differences in pH value, oxygen tension, and nutrient flow, which contribute for the development of tumor resistance to chemotherapy, due to an irregular distribution of the drug through the tissue.[45]

During the experiments, the animals were weighed and observed for possible signs of toxicity. After 15 days of treatment, no signs of toxicity or significant weight loss were observed in animals treated with goniothalamin (**1**), aza-goniothalamin (**2**), or 5-FU. However, animals treated with derivative **18** lost body weight and had an increase in relative liver weight, which could be a sign of toxicity (Figure 8C and D). Thus, in addition to losing its activity when administered in vivo, derivative **18** seems to show signs of toxicity. On the other hand, aza-goniothalamin (**2**) exhibited an in vivo antitumor activity profile similar to that of goniothalamin (**1**), without signs of toxicity being observed. The Ehrlich tumor produces changes in the medullary hematopoietic response of the host, such as anemia, thymic depletion, immunosuppression, and granulocyte-dependent leukocytosis.[46] In the experiments performed, tumor growth was responsible for a decrease in the number of leukocytes (white blood cells, WBC) in all animals, with no differences between groups bearing Ehrlich tumors (see Figure S103 in the Supporting Information).

The surprising results observed for the in vivo experiments may be accounted for by the phase I biotransformations that aza-goniothalamin (**2**) may undergo. Oxidation by enzymes such as cytochrome P450 (CYP), flavine monooxygenase (FMO), or monamine oxidase (MAO) may occur to produce a hyroxylated derivative of aza-goniothalamin; this product may then be converted into the corresponding 2-pyridone derivative, which is an important component of many pharmacological active substances including some antitumor compounds such as camptothecin[47] and fredericamycin A,[48] among others.

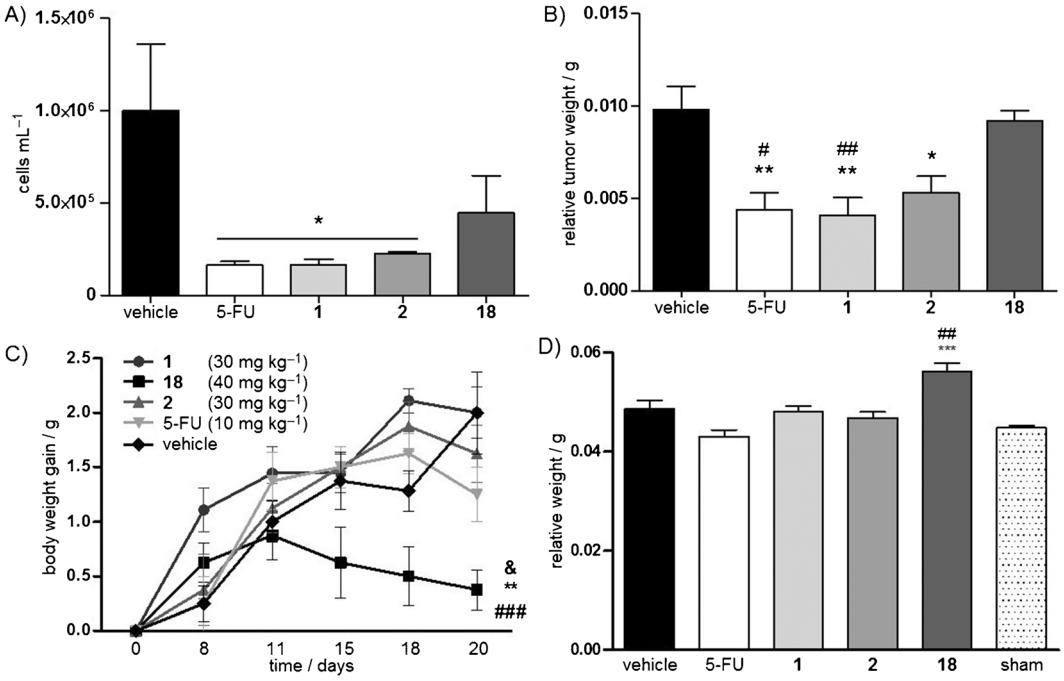

Figure 8. In vivo antitumor activity of goniothalamin (**1**), aza-goniothalamin (**2**), and derivative **18** on Ehrlich tumors in mice. A) Ehrlich ascitic carcinoma: Groups were treated daily (for seven days) by intraperitoneal (i.p.) injection with vehicle (phosphate-buffered saline, PBS), 5-fluorouracil (5-FU, 10 mg kg^{-1}), **1**, **18**, and **2** (50 mg kg^{-1}). Significant antiproliferative activity was observed in animals treated with 5-FU, **1**, and **2** ($^{*}p < 0.05$), relative to that of the vehicle group. B) Ehrlich solid tumor: Groups were treated daily (for 15 days) by i.p. injection with vehicle (PBS), 5-FU (10 mg kg^{-1}), **1** and **2** (30 mg kg^{-1}), and **18** (40 mg kg^{-1}). Significant antiproliferative activity was observed in animals treated with 5-FU and **1** ($^{**}p < 0.01$) or **2** ($p < 0.05$) relative to that of the vehicle group. A significant difference was also observed between treatments with **1** ($^{\#\#}p < 0.01$) and 5-FU ($^{\#}p < 0.05$) relative to the results with **18**. No antiproliferative activity was observed in animals treated with **18**. C) Body weight variation of all groups during the Ehrlich solid tumor model: Animals treated with **18** (40 mg kg^{-1}) presented weight loss, which was statistically different from animals treated with the vehicle ($^{\&}p < 0.05$), **2** ($^{**}p < 0.01$), and **1** ($^{\#\#\#}p < 0.001$). D) Relative liver weight: Animals treated with **18** (40 mg kg^{-1}) presented an increase in relative liver weight, which may be indicative of toxicity. Values were statistically different from those with the vehicle ($^{\#\#}p < 0.01$) and the sham group ($^{***}p < 0.001$). Statistical analysis by Tukey's multiple comparison test and ANOVA.

The toxicity displayed by most available drugs in cancer chemotherapy and radiotherapy is also a major challenge for the development of new drugs that target higher therapeutic indices with selectivity for tumor cell lines.[44] Thus, the absence of signs of toxicity at effective doses of goniothalamin (**1**) and aza-goniothalamin (**2**) is a positive indication for the continuity of preclinical studies with these molecules.

3. Conclusions

In this work, the synthesis and SAR of a focused library of N-acylated aza-goniothalamin derivatives and the in vitro evaluation of the compounds against a panel of eight human cancer cell lines was described. As we anticipated, N-acylation of aza-goniothalamin (**2**) restored the in vitro antiproliferative activity of this family of compounds, which once again confirmed the importance of the Michael acceptor core for the cytotoxic activity of goniothalamin (**1**) and related compounds. Moreover, the presence of methoxy groups at specific positions in the aromatic ring of the styryl side chain significantly enhanced the antiproliferative activity and led to more potent derivatives. Interestingly, derivative **18**, bearing a second Michael acceptor unit, was more potent than the parent molecule and resulted in low TGI values for most of the tumor cell lines evaluated. This could be a consequence of its double Michael acceptor ability in the biological system, as verified by NMR studies with GSH as a representative thiol nucleophile. Owing to the higher potency of derivative **18**, this compound was selected for preliminary mechanistic studies on the PC-3 prostate tumor cell line. Goniothalamin (**1**) and derivative **18** led to ROS generation in PC-3 cells, which probably signals for caspase-dependent apoptosis. Both molecules might interact with glutathione and, thereby, stabilize the intrinsic mechanisms of ROS scavenging. Treatment with derivative **18** also led to G_2/M cell-cycle arrest, which can be directly related to cell death or represents an additional antiproliferative mechanism. The in vivo studies in the Ehrlich ascitic and solid tumor models in mice confirmed the antitumor activity of goniothalamin (**1**), without signs of toxicity. Surprisingly and contrary to its in vitro profile, aza-goniothalamin (**2**) inhibited Ehrlich tumor cell proliferation, both in the ascitic and solid forms, which may be due to an in vivo metabolism that favors its activity. Derivative **18** exhibited an unexpectedly lower in vivo antitumor activity, despite the treatments being conducted at the same site of inoculation (i.p. administration) in the ascitic model. In summary, the absence of signs of toxicity at effective doses of goniothalamin (**1**) and its aza analogue **2** is a positive indication for the continuity of preclinical studies with these molecules. Further in vivo studies approaching the pharmacokinetics of aza-goniothalamin (**2**) will be conducted to unveil the mechanism of its

unexpected in vivo activation. Our findings also highlight the importance of in vivo studies in the search for new candidates for cancer treatment.

Experimental Section

Chemistry

General procedures: Reagents and solvents were commercial grade and were used as supplied, except when specified in the experimental procedure. Et_3N and CH_2Cl_2 were distilled from calcium hydride, and THF was distilled from Na/benzophenone. Reactions were monitored by TLC analysis with Merck silica gel 60 F-254 thin layer plates. Flash column chromatography was performed on Acros silica gel 60 (0.040–0.063 mm). ^{1}H NMR and ^{13}C NMR data were recorded on Bruker Avance (250 MHz for ^{1}H and 62.9 MHz for ^{13}C NMR spectroscopy) spectrometers by using as an internal standard the residual nondeuterated solvent ($CHCl_3$) or tetramethylsilane (^{1}H NMR spectroscopy). Data are reported as follows: chemical shift (δ) in ppm, multiplicity (s: singlet, d: doublet, t: triplet, q: quartet, quint: quintet, sext: sextet, m: multiplet, br: broad signal, app: apparent signal), coupling constant (J) in Hz, integration. High-resolution mass spectra for novel compounds were measured on a Waters XEVO Q-TOF spectrometer (ESI) or in a Waters GCT Premier (EI) spectrometer. Infrared spectra (IR) were obtained on ABB Bomem MB Series B102, Thermo-Nicolet IR-200 or iS5 spectrometers, and absorptions are reported in reciprocal centimeters. Melting points were recorded on an Electrothermal 9100 melting point apparatus and were uncorrected. The purity of all final compounds was higher than 95% and was determined by HPLC.

(*E*)-*N*-(But-3-enyl)but-2-enamide (8): Et_3N (2.0 equiv; 7.5 mmol; 1.05 mL), catalytic DMAP, and crotonyl chloride (**7**; 1.2 equiv; 3.6 mmol; 376 mg) were added successively to a stirred solution of 3-butenylamine hydrochloride (**6**; 3.0 mmol; 323 mg) in anhydrous dichloromethane (5.0 mL) at 0 °C under a nitrogen atmosphere. The reaction mixture was maintained at room temperature for 2 h with stirring. After this period, CH_2Cl_2 (50 mL) and a saturated aqueous solution of sodium hydrogen carbonate (20 mL) were added. The organic layer was separated and washed successively with 3% HCl aqueous solution (20 mL) and 5% sodium hydrogen carbonate aqueous solution (20 mL). The organic layer was dried over anhydrous sodium sulfate, filtered, and concentrated under reduced pressure. The crude residue was purified by flash column chromatography (hexanes/ethyl acetate, 1:1 *v/v*) to give the corresponding amide **8** in 79% yield, as a colorless viscous oil. IR (thin film): $\tilde{\nu}$ = 3285, 3079, 2917, 1672, 1630, 1550, 1445, 1340, 1289, 1231, 968, 913 cm^{-1}; ^{1}H NMR (250 MHz, $CDCl_3$): δ = 6.80 (sext, J = 6.8 Hz, 1H), 6.63 (br s, 1H), 5.90 (dd, J = 15.2, 1.4 Hz, 1H), 5.83–5.69 (m, 1H), 5.09 (d, J = 11.4 Hz, 1H), 5.03 (d, J = 3.6 Hz, 1H), 3.36 (q, J = 6.8 Hz, 2H), 2.28 (q, J = 6.8 Hz, 2H), 1.83 ppm (dd, J = 6.8, 1.2 Hz, 3H); ^{13}C NMR (62.9 MHz, $CDCl_3$): δ = 166.1 (C_0), 138.9 (CH), 135.1 (CH), 125.2 (CH), 116.6 (CH_2), 38.4 (CH_2), 33.5 (CH_2), 17.4 ppm (CH_3); HRMS (ESI+): *m/z* calcd for $C_8H_{14}NO$ [$M+H^+$]: 140.1075; found: 140.1118.

5,6-Dihydropyridin-2(1*H*)-one (9): Grubbs second-generation catalyst (2.5 mol%; 0.03 mmol; 25 mg) was added to a solution of amide **8** (1.19 mmol; 165 mg) in dry CH_2Cl_2 (120 mL) with heating at reflux and magnetic stirring. After 2 h under these conditions, the reaction was allowed to cool to room temperature, and the solvent was removed under reduced pressure. The residue obtained was subjected to flash column chromatography (ethyl acetate with 1% Et_3N *v/v*) to afford the corresponding lactam **9** in 94% yield, as a light brown viscous oil, which solidified after standing. IR (thin film): $\tilde{\nu}$ = 3216, 3053, 2934, 1664, 1606, 1489, 1425, 1339, 1313, 1138, 810 cm^{-1}; ^{1}H NMR (250 MHz, $CDCl_3$): δ = 7.46 (br s, 1H), 6.68–6.64 (m, 1H), 5.88 (d, J = 9.9 Hz, 1H), 3.45–3.39 (m, 2H), 2.35–2.33 ppm (m, 2H); ^{13}C NMR (62.9 MHz, $CDCl_3$): δ = 166.5 (C_0), 141.2 (CH), 124.4 (CH), 39.0 (CH_2), 23.4 ppm (CH_2); HRMS (ESI+): *m/z* calcd for C_5H_8NO [$M+H^+$]: 98.0606; found: 98.0641.

(*E*)-3-(3,4,5-Trimethoxyphenyl)acrylic acid (12): A solution of 3,4,5-trimethoxybenzaldehyde (**10**; 51.0 mmol; 10.0 g), malonic acid (**11**; 2.18 equiv; 111.2 mmol; 11.6 g) in anhydrous pyridine (5.7 equiv; 291.0 mmol; 24 mL), and anhydrous piperidine (0.2 equiv; 10.2 mmol; 1.0 mL) was heated at reflux for 2 h. After cooling to room temperature, the reaction mixture was added to an aqueous solution of hydrogen chloride 5% (500 mL), chilled, and filtered under reduced pressure. The precipitate was dissolved in ethyl acetate (350 mL) and washed with water (2×100 mL). The organic layer was dried over anhydrous sodium sulfate, filtered, and concentrated under reduced pressure. The crude residue was purified by flash column chromatography (hexanes/ethyl acetate, 1:1 *v/v*) to afford the *trans*-3,4,5-trimethoxycinnamic acid (**12**) in 87% yield, as a white solid; mp: 127.0–129.0 °C; IR (thin film): $\tilde{\nu}$ = 3350–2500, 3106, 3005, 2948, 2839, 1689, 1626, 1584, 1504, 1455, 1397, 1341, 1285, 1247, 1203, 1120, 998, 828 cm^{-1}; ^{1}H NMR (250 MHz, $CDCl_3$): δ = 11.5 (br s, 1H), 7.70 (d, J = 15.8 Hz, 1H), 6.77 (s, 2H), 6.35 (d, J = 15.8 Hz, 1H), 3.88 ppm (s, 9H); ^{13}C NMR (62.9 MHz, $CDCl_3$): δ = 172.5 (C_0), 153.4 (2×C_0), 147.0 (CH), 140.5 (C_0), 129.4 (C_0), 116.4 (CH), 105.5 (2×CH), 60.9 (OCH_3), 56.1 ppm (2×OCH_3); HRMS (ESI+): *m/z* calcd for $C_{12}H_{15}O_5$ [$M+H^+$]: 239.0919; found: 239.0984.

(*E*)-1-(3-(3,4,5-Trimethoxyphenyl)acryloyl)-5,6-dihydropyridin-2(1*H*)-one (piplartine; 3): Oxalyl chloride (1.2 equiv; 2.73 mmol; 0.24 mL) and catalytic DMF were added dropwise to a stirred solution of (*E*)-3-(3,4,5-trimethoxyphenyl)acrylic acid (**12**; 1.1 equiv; 2.27 mmol; 541 mg) in anhydrous dichloromethane (5.0 mL), at 0 °C. The reaction was stirred while being slowly warmed to room temperature for 2 h. After this period, the volatiles were removed under reduced pressure, and the crude residue was dissolved in anhydrous THF (10 mL). Anhydrous Et_3N (2.0 equiv; 4.12 mmol; 0.58 mL) and catalytic DMAP were added to the solution, and the mixture was stirred for 15 min at 0 °C. Next, a solution of lactam **9** (1.0 equiv; 2.06 mmol; 200 mg) in anhydrous THF (10 mL) was carefully added, and the resulting solution was stirred at room temperature for 40 h. After this period, the reaction mixture was diluted with CH_2Cl_2 (50 mL), washed successively with saturated ammonium chloride aqueous solution (25 mL) and brine (25 mL), dried over anhydrous sodium sulfate, filtered, and concentrated under reduced pressure. The residue obtained was purified by flash column chromatography (petroleum ether/ethyl acetate, 2:1, 1.5:1, 1:1 *v/v*) to afford piplartine (**3**) in 67% yield (white solid); mp: 125.0–127.0 °C (lit.: 120.0–121.0 °C, 122.2–122.6 °C, 124.0 °C, 123.0–124.0 °C, 128.0–130.0 °C); IR (thin film): $\tilde{\nu}$ = 2963, 2945, 2927, 2832, 1682, 1619, 1586, 1508, 1425, 1326, 1179, 1130, 1118, 1003, 963, 819 cm^{-1}; ^{1}H NMR (250 MHz, $CDCl_3$): δ = 7.62 (d, J = 15.6 Hz, 1H), 7.38 (d, J = 15.6 Hz, 1H), 6.93–6.86 (m, 1H), 6.76 (s, 2H), 5.99 (d, J = 9.7 Hz, 1H), 3.99 (t, J = 6.5 Hz, 2H), 3.84 (s, 6H), 3.83 (s, 3H), 2.46–2.40 ppm (m, 1H); ^{13}C NMR (62.9 MHz, $CDCl_3$): δ = 168.7 (C_0), 165.7 (C_0), 153.2 (2×C_0), 145.4 (CH), 143.5 (CH), 139.8 (C_0), 130.5 (C_0), 125.6 (CH), 121.0 (CH), 105.3 (2×CH), 60.8 (OCH_3), 56.0 (2×OCH_3), 41.5 (CH_2), 24.6 ppm (CH_2); HRMS (ESI+): *m/z* calcd for $C_{17}H_{20}NO_5$ [$M+H^+$]: 318.1341: found: 318.1358.

General procedure for the N-acylation by using acyl chloride or methyl chloroformate and LHMDS: A solution of LHMDS (1 M in

THF; 1.3 equiv; 0.65 mmol) was carefully added to a solution of the lactams **2** or **26--31** (0.5 mmol; 100 mg) in anhydrous THF (3.8 mL), at −78 °C with magnetic stirring and under a nitrogen atmosphere. After 15 min under these conditions, a solution of the appropriate acyl chloride (2.0 equiv; 1.0 mmol) in anhydrous THF (1.2 mL) was added dropwise. The reaction mixture was maintained at −78 °C for 1 h and then left standing at room temperature for 1 h. Next, the mixture was diluted with ethyl acetate (30 mL) and washed with a saturated sodium hydrogen carbonate aqueous solution (20 mL). The layers were separated, and the aqueous layer was extracted twice with ethyl acetate (30 mL). The combined organic layer was dried over anhydrous sodium sulfate, filtered, and concentrated under reduced pressure. The residue obtained was purified by flash column chromatography (by using the solvent indicated) to afford the *N*-acyl-aza-goniothalamin derivatives **13**–**16, 18, 19**, and **32**–**37**.

(*E*)-Methyl 2-oxo-6-styryl-5,6-dihydropyridine-1(2*H*)-carboxylate (13): Prepared according to the general procedure for the N-acylation by using methyl chloroformate and LHMDS in 98% yield (white solid). Eluent: hexanes/ethyl acetate, 1:1, 1:2 *v/v*; mp: 94.0–95.0 °C; IR (thin film): $\tilde{\nu}$ = 2953, 2922, 2850, 1711, 1697, 1437, 1393, 1287, 1233, 1132, 1085, 967, 952, 813, 757, 698 cm^{-1}; ^1H NMR (250 MHz, $CDCl_3$): δ = 7.35–7.21 (m, 5H), 6.69 (t, J = 7.7 Hz, 1H), 6.54 (d, J = 15.9 Hz, 1H), 6.23 (dd, J = 15.9, 6.1 Hz, 1H), 6.03 (dd, J = 9.8, 2.6 Hz, 1H), 5.31 (t, J = 4.2 Hz, 1H), 3.90 (s, 3H), 2.97–2.87 (m, 1H), 2.50 ppm (dd, J = 18.4, 6.3 Hz, 1H); ^{13}C NMR (62.9 MHz, $CDCl_3$): δ = 162.8 (C_0), 154.6 (C_0), 141.1 (CH), 135.8 (C_0), 132.0 (CH), 128.5 (2×CH), 127.9 (CH), 126.5 (CH), 126.4 (2×CH), 125.8 (CH), 55.2 (OCH_3), 53.9 (CH), 29.7 ppm (CH_2); HRMS (ESI+): *m/z* calcd for $C_{15}H_{16}NO_3$ [$M+H^+$]: 258.1130; found: 258.1186.

(*E*)-1-Acetyl-6-styryl-5,6-dihydropyridin-2(1*H*)-one (14): Prepared according to the general procedure for the N-acylation by using acetyl chloride and LHMDS in 85% yield (white solid). Eluent: hexanes/ethyl acetate, 2:1 *v/v*; mp: 90.0–92.0 °C; IR (thin film): $\tilde{\nu}$ = 2918, 1694, 1682, 1632, 1393, 1369, 1352, 1232, 1140, 1021, 966, 819, 703 cm^{-1}; ^1H NMR (250 MHz, $CDCl_3$): δ = 7.35–7.19 (m, 5H), 6.79 (t, J = 7.9 Hz, 1H), 6.49 (d, J = 15.9 Hz, 1H), 6.19 (dd, J = 15.9, 6.2 Hz, 1H), 6.05 (dd, J = 9.8, 2.8 Hz, 1H), 5.63 (t, J = 6.2 Hz, 1H), 2.91–2.78 (m, 1H), 2.61 (s, 3H), 2.54 ppm (dd, J = 19.2, 6.8 Hz, 1H); ^{13}C NMR (62.9 MHz, $CDCl_3$): δ = 172.7 (C_0), 164.9 (C_0), 142.4 (CH), 136.0 (C_0), 132.0 (CH), 128.5 (2×CH), 127.8 (CH), 126.6 (CH), 126.4 (2×CH), 125.7 (CH), 51.9 (CH), 29.6 (CH_2), 27.5 ppm (CH_3); HRMS (ESI+): *m/z* calcd for $C_{15}H_{15}NNaO_2$ [$M+Na^+$]: 264.0995; found: 264.0968.

(*E*)-1-(2-Bromoacetyl)-6-styryl-5,6-dihydropyridin-2(1*H*)-one (15): Prepared according to the general procedure for the N-acylation by using 2-bromoacetyl chloride and LHMDS in 58% yield (orange solid). Eluent: hexanes/ethyl acetate, 3:1 *v/v*; mp: 126.0–128.0 °C; IR (thin film): $\tilde{\nu}$ = 3057, 2950, 2923, 1703, 1674, 1609, 1448, 1414, 1329, 1318, 1176, 1128, 1027, 964, 819, 810, 756, 696 cm^{-1}; ^1H NMR (250 MHz, $CDCl_3$): δ = 7.40–7.20 (m, 5H), 6.85 (t, J = 7.5 Hz, 1H), 6.54 (d, J = 15.9 Hz, 1H), 6.18 (dd, J = 15.9, 6.3 Hz, 1H), 6.07 (dd, J = 9.7, 2.7 Hz, 1H), 5.78 (t, J = 6.3 Hz, 1H), 4.64 (d, J = 1.5 Hz, 2H), 2.97–2.82 (m, 1H), 2.56 ppm (dd, J = 18.8, 6.2 Hz, 1H); ^{13}C NMR (62.9 MHz, $CDCl_3$): δ = 168.5 (C_0), 164.5 (C_0), 143.4 (CH), 135.7 (C_0), 132.8 (CH), 128.5 (2×CH), 128.1 (CH), 126.5 (2×CH), 125.5 (CH), 125.0 (CH), 53.3 (CH), 33.5 (CH_2), 29.6 ppm (CH_2); HRMS (EI): *m/z* calcd for $C_{15}H_{14}NO_2$ [$M^+-Br^•$]: 240.1019; found: 240.0993.

(*E*)-1-(2-Chloroacetyl)-6-styryl-5,6-dihydropyridin-2(1*H*)-one (16): Prepared according to the general procedure for the N-acylation by using 2-chloroacetyl chloride and LHMDS in 68% yield (white solid). Eluent: hexanes/ethyl acetate, 3:1 *v/v*; mp: 107.7–109.5 °C; IR (thin film): $\tilde{\nu}$ = 3027, 2972, 1692, 1683, 1393, 1354, 1333, 1320, 1205, 1142, 1035, 967, 822 cm^{-1}; ^1H NMR (250 MHz, $CDCl_3$): δ = 7.38–7.20 (m, 5H), 6.91–6.77 (m, 1H), 6.54 (dd, J = 15.0, 2.5 Hz, 1H), 6.18 (dd, J = 15.0, 7.5 Hz, 1H), 6.06 (dd, J = 10.0, 2.5 Hz, 1H), 5.59 (td, J = 7.5, 2.5 Hz, 1H), 4.81 (q, J = 17.5 Hz, 2H), 2.87 (ddt, J = 18.8, 6.5, 2.5 Hz, 1H), 2.56 ppm (dd, J = 18.8, 6.2 Hz, 1H); ^{13}C NMR (62.9 MHz, $CDCl_3$): δ = 168.9 (C_0), 164.5 (C_0), 143.5 (CH), 135.7 (C_0), 132.9 (CH), 128.5 (2×CH), 128.0 (CH), 126.5 (2×CH), 125.4 (CH), 124.9 (CH), 53.2 (CH), 47.4 (CH_2), 29.5 ppm (CH_2); HRMS (EI): *m/z* calcd for $C_{15}H_{14}NO_2$ [$M^+-Cl^•$]: 240.1019; found: 240.0997.

1-(*E*)-But-2-enoyl-6-styryl-5,6-dihydropyridin-2(1*H*)-one (18): Prepared according to the general procedure for the N-acylation by using crotonyl chloride and LHMDS in 82% yield (light yellow solid). Eluent: hexanes/ethyl acetate, 3:1 *v/v*; mp: 89.0–91.0 °C; IR (thin film): $\tilde{\nu}$ = 3034, 2983, 2917, 2850, 1684, 1670, 1630, 1388, 1358, 1325, 1197, 1141, 969, 812, 755, 696 cm^{-1}; ^1H NMR (250 MHz, $CDCl_3$): δ = 7.34–7.14 (m, 5H), 7.11–6.93 (m, 1H), 6.86 (dd, J = 17.5, 2.5 Hz, 1H), 6.75–6.64 (m, 1H), 6.45 (d, J = 15.0 Hz, 1H), 6.15 (dd, J = 15.0, 5.0 Hz, 1H), 5.98 (dd, J = 10.0, 2.5 Hz, 1H), 5.46 (t, J = 5.0 Hz, 1H), 2.85–2.67 (m, 1H), 2.46 (dd, J = 17.5, 5.0 Hz, 1H), 1.39 ppm (dd, J = 7.5, 2.5 Hz, 3H); ^{13}C NMR (62.9 MHz, $CDCl_3$): δ = 167.9 (C_0), 164.9 (C_0), 143.2 (CH), 142.4 (CH), 135.8 (C_0), 131.5 (CH), 128.2 (2×CH), 127.5 (CH), 126.7 (CH), 126.2 (2×CH), 125.9 (CH), 125.4 (CH), 52.4 (CH), 29.5 (CH_2), 18.0 ppm (CH_3); HRMS (ESI+): *m/z* calcd for $C_{17}H_{18}NO_2$ [$M+H^+$]: 268.1338; found: 268.1388.

1-Cinnamoyl-6-styryl-5,6-dihydropyridin-2(1*H*)-one (19): Prepared according to the general procedure for the N-acylation by using cinnamoyl chloride and LHMDS in 67% yield (light yellow solid). The cinnamoyl chloride was prepared from dropwise addition of oxalyl chloride (3.89 equiv) to a solution of cinnamic acid (1.0 equiv) in anhydrous dichloromethane (0.3 M) and DMF (1 drop). After concentration to dryness, the crude product was used directly in the next reaction. Eluent: hexanes/ethyl acetate, 4:1, 3:1 *v/v*; mp: 105.7–106.5 °C; IR (thin film): $\tilde{\nu}$ = 3058, 2921, 2851, 1688, 1671, 1624, 1576, 1394, 1333, 1202, 1142, 965, 819, 761, 753 cm^{-1}; ^1H NMR (250 MHz, $CDCl_3$): δ = 7.78 (d, J = 15.6 Hz, 1H), 7.57–7.51 (m, 3H), 7.37–7.18 (m, 8H), 6.78 (t, J = 7.4 Hz, 1H), 6.53 (d, J = 15.9 Hz, 1H), 6.22 (dd, J = 15.9, 5.9 Hz, 1H), 6.06 (dd, J = 9.8, 2.6 Hz, 1H), 5.59 (t, J = 5.9 Hz, 1H), 2.92–2.82 (m, 1H), 2.55 ppm (dd, J = 18.7, 6.3 Hz, 1H); ^{13}C NMR (62.9 MHz, $CDCl_3$): δ = 168.4 (C_0), 165.3 (C_0), 143.7 (CH), 142.6 (CH), 136.0 (C_0), 135.0 (C_0), 132.0 (CH), 130.0 (CH), 128.7 (2×CH), 128.4 (2×CH), 128.2 (2×CH), 127.8 (CH), 126.7 (CH), 126.5 (2×CH), 125.8 (CH), 121.7 (CH), 52.8 (CH), 29.8 ppm (CH_2); HRMS (ESI+): *m/z* calcd for $C_{22}H_{20}NO_2$ [$M+H^+$]: 330.1494; found: 330.1482.

1-(*E*)-But-2-enoyl-6-(4-methoxystyryl)-5,6-dihydropyridin-2(1*H*)-one (32): Prepared according to the general procedure for the N-acylation by using crotonyl chloride and LHMDS in 55% yield (light yellow solid). Eluent: hexanes/ethyl acetate, 2:1 *v/v*; mp: 105.0–107.0 °C; IR (thin film): $\tilde{\nu}$ = 2955, 2931, 2856, 2837, 1685, 1636, 1607, 1512, 1389, 1326, 1293, 1248, 1201, 1176, 1137, 1033, 964, 839, 816 cm^{-1}; ^1H NMR (250 MHz, $CDCl_3$): 7.24 (d, J = 8.7 Hz, 2H), 7.13–6.96 (m, 1H), 6.92–6.71 (m, 4H), 6.44 (d, J = 15.9 Hz, 1H), 6.12–5.97 (m, 2H), 5.49 (t, J = 5.9 Hz, 1H), 3.77 (s, 3H), 2.92–2.76 (m, 1H), 2.51 (dd, J = 18.6, 6.1 Hz, 1H), 1.97 ppm (dd, J = 6.7, 1.0 Hz, 3H); ^{13}C NMR (62.9 MHz, $CDCl_3$): δ = 168.3 (C_0), 165.3 (C_0), 159.3 (C_0), 143.6 (CH), 142.5 (CH), 131.4 (CH), 128.9 (C_0), 127.7 (2×CH), 126.1 (CH), 125.8 (CH), 124.5 (CH), 113.9 (2×CH), 55.2 (OCH_3), 52.8 (CH), 30.0 (CH_2), 18.3 ppm (CH_3); HRMS (ESI+): *m/z* calcd for $C_{18}H_{20}NO_3$ [$M+H^+$]: 298.1443; found: 298.1412.

1-(*E*)-But-2-enoyl-6-(2,4-dimethoxystyryl)-5,6-dihydropyridin-2(1*H*)-one (33): Prepared according to the general procedure for the N-acylation by using crotonyl chloride and LHMDS in 63% yield (yellow solid). Eluent: hexanes/ethyl acetate, 2:1 *v/v*; mp: 87.5–89.0 °C; IR (thin film): $\tilde{\nu}$ = 3045, 3005, 2969, 2926, 2848, 1680, 1638, 1604, 1507, 1395, 1330,1296, 1280, 1205, 1143, 1106, 1027, 966, 937, 834, 812 cm^{-1}; ^1H NMR (250 MHz, $CDCl_3$): δ = 7.24 (d, J = 7.5 Hz, 1H), 7.12–6.95 (m, 1H), 6.86 (dd, J = 15.0, 2.5 Hz, 1H), 6.81–6.67 (m, 2H), 6.44–6.35 (m, 2H), 6.13 (dd, J = 15.0, 7.5 Hz, 1H), 6.02 (dd, J = 10.0, 2.5 Hz, 1H), 5.48 (t, J = 7.5 Hz, 1H), 3.77 (s, 6H), 2.89–2.73 (m, 1H), 2.55 (dd, J = 17.5, 7.5 Hz, 1H), 1.92 ppm (dd, J = 7.5, 2.5 Hz, 3H); ^{13}C NMR (62.9 MHz, $CDCl_3$): δ = 168.3 (C_0), 165.3 (C_0), 160.5 (C_0), 157.9 (C_0), 143.3 (CH), 142.7 (CH), 127.8 (CH), 126.7 (CH), 126.2 (CH), 125.7 (CH), 125.0 (CH), 118.2 (C_0), 104.6 (CH), 98.3 (CH), 55.4 (OCH_3), 55.3 (OCH_3), 53.3 (CH), 30.0 (CH_2), 18.2 ppm (CH_3); HRMS (ESI+): *m/z* calcd for $C_{19}H_{22}NO_4$ [$M+H^+$]: 328.1549; found: 328.1561.

1-(*E*)-But-2-enoyl-6-(3,4-dimethoxystyryl)-5,6-dihydropyridin-2(1*H*)-one (34): Prepared according to the general procedure for the N-acylation by using crotonyl chloride and LHMDS in 51% yield (yellow oil). Eluent: hexanes/ethyl acetate, 2:1 *v/v*. IR (thin film): $\tilde{\nu}$ = 2955, 2932, 2925, 2851, 1685, 1636, 1515, 1419, 1389, 1327, 1264, 1200, 1139, 1026, 963, 814, 766 cm^{-1}; ^1H NMR (250 MHz, $CDCl_3$): δ = 7.13–6.98 (m, 1H), 6.91–6.73 (m, 5H), 6.42 (d, J = 15.8 Hz, 1H), 6.12–5.99 (m, 2H), 5.50 (t, J = 5.6 Hz, 1H), 3.86 (s, 3H), 3.85 (s, 3H), 2.93–2.77 (m, 1H), 2.54 (dd, J = 18.8, 5.8 Hz, 1H), 1.93 ppm (dd, J = 7.5, 2.5 Hz, 3H); ^{13}C NMR (62.9 MHz, $CDCl_3$): δ = 168.3 (C_0), 165.4 (C_0), 149.0 (C_0), 143.7 (CH), 142.6 (CH), 131.7 (CH), 129.2 (C_0), 126.1 (CH), 125.9 (CH), 124.8 (CH), 119.7 (CH), 111.0 (CH), 109.0 (CH), 55.9 (OCH_3), 55.8 (OCH_3), 52.8 (CH), 29.9 (CH_2), 18.3 ppm (CH_3); HRMS (ESI+): *m/z* calcd for $C_{19}H_{22}NO_4$ [$M+H^+$]: 328.1549; found: 328.1561.

1-(*E*)-But-2-enoyl-6-(3,5-dimethoxystyryl)-5,6-dihydropyridin-2(1*H*)-one (35): Prepared according to the general procedure for the N-acylation by using crotonyl chloride and LHMDS in 70% yield (white solid). Eluent: hexanes/ethyl acetate, 2:1 *v/v*; mp: 340 °C (decomp.); IR (thin film): $\tilde{\nu}$ = 2960, 2922, 2851, 1684, 1592, 1389, 1327, 1294, 1203, 1152, 1136, 1091, 1066, 962, 809 cm^{-1}; ^1H NMR (250 MHz, $CDCl_3$): δ = 7.14–6.96 (m, 1H), 6.86 (dd, J = 15.2, 1.2 Hz, 1H), 6.81–6.71 (m, 1H), 6.48–6.31 (m, 4H), 6.15 (dd, J = 15.8, 5.7 Hz, 1H), 6.03 (dd, J = 9.8, 2.7 Hz, 1H), 5.50 (t, J = 5.6 Hz, 1H), 3.76 (s, 6H), 2.92–2.75 (m, 1H), 2.53 (dd, J = 18.6, 6.1 Hz, 1H), 1.93 ppm (dd, J = 6.6, 1.1 Hz, 3H); ^{13}C NMR (62.9 MHz, $CDCl_3$): δ = 168.3 (C_0), 165.3 (C_0), 160.8 (2×C_0), 143.8 (CH), 142.5 (CH), 138.1 (C_0), 131.9 (CH), 127.4 (CH), 126.1 (CH), 125.9 (CH), 104.5 (2×CH), 100.4 (CH), 55.3 (2×OCH_3), 52.6 (CH), 29.8 (CH_2), 18.3 ppm (CH_3); HRMS (ESI+): *m/z* calcd for $C_{19}H_{22}NO_4$ [$M+H^+$]: 328.1549; found: 328.1561.

1-(*E*)-But-2-enoyl-6-(3,4,5-trimethoxystyryl)-5,6-dihydropyridin-2(1*H*)-one (36): Prepared according to the general procedure for the N-acylation by using crotonyl chloride and LHMDS in 78% yield (white solid). Eluent: hexanes/ethyl acetate, 2:1 *v/v*; mp: 80.0–82.0 °C; IR (thin film): $\tilde{\nu}$ = 3002, 2928, 2860, 2827, 1690, 1676, 1583, 1508, 1421, 1390, 1325, 1242, 1195, 1125, 1007, 968 cm^{-1}; ^1H NMR (250 MHz, $CDCl_3$): δ = 7.13–6.96 (m, 1H), 6.92–6.73 (m, 2H), 6.42 (s, 2H), 6.44–6.33 (m, 1H), 6.14–5.98 (m, 2H), 5.49 (t, J = 7.5 Hz, 1H), 3.83 (s, 6H), 3.80 (s, 3H), 2.93–2.77 (m, 1H), 2.54 (dd, J = 17.5, 7.5 Hz, 1H), 1.93 ppm (d, J = 7.5 Hz, 3H); ^{13}C NMR (62.9 MHz, $CDCl_3$): δ = 168.2 (C_0), 165.3 (C_0), 153.2 (2×C_0), 143.7 (CH), 142.5 (CH), 138.0 (C_0), 131.8 (CH), 131.7 (CH), 126.2 (CH), 126.0 (CH), 125.8 (C_0), 103.6 (2×CH), 60.8 (OCH_3), 56.0 (2×OCH_3), 52.6 (CH), 29.8 (CH_2), 18.3 ppm (CH_3); HRMS (ESI+): *m/z* calcd for $C_{20}H_{24}NO_5$ [$M+H^+$]: 358.1654; found: 358.1580.

1-(*E*)-But-2-enoyl-6-(2,4,5-trimethoxystyryl)-5,6-dihydropyridin-2(1*H*)-one (37): Prepared according to the general procedure for the N-acylation by using crotonoyl chloride and LHMDS in 53% yield (white solid). Eluent: hexanes/ethyl acetate, 2:1 *v/v*; mp: 121.0–122.4 °C; IR (thin film): $\tilde{\nu}$ = 2955, 2926, 2846, 1684, 1637, 1508, 1464, 1440, 1390, 1324, 1291, 1206, 1136, 1097, 1032, 965, 868, 814 cm^{-1}; ^1H NMR (250 MHz, $CDCl_3$): δ = 7.10–6.93 (m, 1H), 6.89–6.68 (m, 4H), 6.43 (s, 1H), 6.08 (dd, J = 16.0, 6.2 Hz, 1H), 6.00 (dd, J = 9.9, 2.5 Hz, 1H), 5.47 (t, J = 5.9 Hz, 1H), 3.83 (s, 3H), 3.80 (s, 3H), 3.75 (s, 3H), 2.89–2.73 (m, 1H), 2.54 (dd, J = 18.5, 6.0 Hz, 1H), 1.89 ppm (d, J = 6.6 Hz, 3H); ^{13}C NMR (62.9 MHz, $CDCl_3$): δ = 168.2 (C_0), 165.3 (C_0), 151.5 (C_0), 149.6 (C_0), 143.3 (CH), 143.1 (C_0), 142.7 (CH), 126.4 (CH), 126.1 (CH), 125.7 (CH), 124.9 (CH), 116.8 (C_0), 110.0 (CH), 97.6 (CH), 56.5 (OCH_3), 56.4 (OCH_3), 55.9 (OCH_3), 53.2 (CH), 29.9 (CH_2), 18.2 ppm (CH_3); HRMS (ESI+): *m/z* calcd for $C_{20}H_{24}NO_5$ [$M+H^+$]: 358.1654; found: 358.1580.

General procedure for the N-acylation by using mixed anhydride and LHMDS: Et_3N (1.6 equiv; 3.2 mmol; 0.45 mL) and pivaloyl chloride (1.2 equiv; 2.4 mmol; 296 μL) were added to a stirred solution of the carboxylic acid of interest (for preparation, see the Supporting Information; 1.2 equiv; 2.4 mmol) in anhydrous THF (20.0 mL), at 0 °C under a nitrogen atmosphere. After 30 min under these conditions, a solution of the lithium salt (the lithium salt was prepared from the addition of LHMDS (1 M in THF; 1.3 equiv; 2.6 mmol; 2.6 mL) to a stirred solution of the aza-goniothalamin (**2**; 1.0 equiv; 2.0 mmol) in anhydrous THF (15 mL) at 0 °C. The reaction mixture was maintained under these conditions for 15 min.) was added through a cannula. After 1 h at 0 °C, the cooling bath was removed, and the reaction mixture was stirred at room temperature for 1 h. Next, the mixture was diluted with ethyl acetate (50 mL) and washed with a saturated aqueous solution of sodium hydrogen carbonate (40 mL). The layers were separated, and the aqueous layer was extracted twice with ethyl acetate (50 mL). The combined organic layer was dried over anhydrous sodium sulfate, filtered, and concentrated under reduced pressure. The residue obtained was purified by flash column chromatography (by using the solvent indicated) to afford the *N*-acyl-aza-goniothalamin analogues **17** and **20**–**22**.

(*E*)-1-Acryloyl-6-styryl-5,6-dihydropyridin-2(1*H*)-one (17): Prepared according to the general procedure for the N-acylation by using mixed anhydride and LHMDS in 53% yield (white solid). Eluent: hexanes/ethyl acetate, 3:1, 2:1 *v/v*; mp: 98.0–99.7 °C; IR (thin film): $\tilde{\nu}$ = 2955, 2922, 2852, 1686, 1672, 1628, 1615, 1391, 1351, 1210, 1140, 966, 821, 793, 757, 697 cm^{-1}; ^1H NMR (250 MHz, $CDCl_3$): δ = 7.34–7.19 (m, 5H), 7.08 (dd, J = 17.0, 10.4 Hz, 1H), 6.81 (t, J = 8.0 Hz, 1H), 6.52 (d, J = 16.0 Hz, 1H), 6.41 (d, J = 17.0 Hz, 1H), 6.20 (dd, J = 16.0, 6.0 Hz, 1H), 6.05 (dd, J = 9.6, 2.6 Hz, 1H), 5.77 (d, J = 10.4 Hz, 1H), 5.53 (t, J = 5.8 Hz, 1H), 2.94–2.84 (m, 1H), 2.56 ppm (dd, J = 18.6, 6.2 Hz, 1H); ^{13}C NMR (62.9 MHz, $CDCl_3$): δ = 168.3 (C_0), 165.0 (C_0), 142.9 (CH), 136.0 (C_0), 132.1 (CH), 131.5 (CH), 128.6 (CH_2), 128.5 (2×CH), 127.9 (CH), 126.5 (2×CH), 126.4 (CH),125.5 (CH), 52.8 (CH), 29.8 ppm (CH_2); HRMS (ESI+): *m/z* calcd for $C_{16}H_{16}NO_2$ [$M+H^+$]: 254.1181; found: 254.1239.

1-((*E*)-3-(3,4-Bis(*tert*-butyldimethylsilyloxy)phenyl)acryloyl)-6-styryl-5,6-dihydropyridin-2(1*H*)-one (20): Prepared according to the general procedure for the N-acylation by using mixed anhydride and LHMDS in 74% yield (white solid). Eluent: hexanes/ethyl acetate, 3:1 *v/v*; mp: 144.0–146.0 °C; IR (thin film): $\tilde{\nu}$ = 2956, 2930, 2893, 2858, 1676, 1622, 1598, 1508, 1392, 1336, 1292, 1253, 1198,

1169, 1136, 984, 917, 839, 824, 786, 688, 668 cm^{-1}; ^1H NMR (250 MHz, $CDCl_3$): $\delta = 7.71$ (d, $J = 15.6$ Hz, 1H), 7.43 (d, $J = 15.6$ Hz, 1H), 7.37–7.20 (m, 5H), 7.16–7.07 (m, 2H), 6.83 (d, $J = 8.2$ Hz, 1H), 6.81–6.72 (m, 1H), 6.54 (d, $J = 15.9$ Hz, 1H), 6.23 (dd, $J = 15.9$, 5.8 Hz, 1H), 6.07 (dd, $J = 9.8$, 2.5 Hz, 1H), 5.62 (t, $J = 5.6$ Hz, 1H), 2.95–2.78 (m, 1H), 2.55 (dd, $J = 18.6$, 6.1 Hz, 1H), 1.02 (s, 9H), 1.01 (s, 9H), 0.24 ppm (br s, 12H); ^{13}C NMR (62.9 MHz, $CDCl_3$): $\delta = 168.5$ (C_0), 165.2 (C_0), 149.1 (C_0), 147.0 (C_0), 144.0 (CH), 142.3 (CH), 136.1 (C_0), 131.9 (CH), 128.7 (C_0), 128.4 (2×CH), 127.7 (CH), 126.8 (CH), 126.4 (2×CH), 125.9 (CH), 122.0 (CH), 121.1 (CH), 121.1 (CH), 119.5 (CH), 52.7 (CH), 29.8 (CH_2), 25.9 (3×CH_3), 25.8 (3×CH_3), 18.4 (C_0), 18.4 (C_0), −4.2 ppm (4×CH_3); HRMS (ESI+): *m/z* calcd for $C_{34}H_{48}NO_4Si_2$ [$M+H^+$]: 590.3122; found: 590.3173.

(*E*)-1-(3-(3,4-Bis(*tert*-butyldimethylsilyloxy)phenyl)propanoyl)-6-styryl-5,6-dihydropyridin-2(1*H*)-one (21): Prepared according to the general procedure for the N-acylation by using mixed anhydride and LHMDS in 76% yield (white solid). Eluent: hexanes/ethyl acetate, 3:1 *v/v*; mp: 91.5–93.0 °C; IR (thin film): $\tilde{\nu} = 2956$, 2929, 2893, 2885, 2856, 1693, 1511, 1390, 1286, 1252, 1187, 1137, 976, 907, 839, 824, 781, 751, 695 cm^{-1}; ^1H NMR (250 MHz, $CDCl_3$): $\delta =$ 7.37–7.20 (m, 5H), 6.80–6.67 (m, 4H), 6.50 (d, $J = 15.8$ Hz, 1H), 6.19 (dd, $J = 15.8$, 6.2 Hz, 1H), 6.03 (dd, $J = 9.8$, 2.5 Hz, 1H), 5.60 (t, $J =$ 5.8 Hz, 1H), 3.45–3.29 (m, 1H), 3.27–3.10 (m, 1H), 3.04–2.70 (m, 3H), 2.50 (dd, $J = 18.6$, 6.1 Hz, 1H), 1.01 (s, 18H), 0.22 (s, 6H), 0.21 ppm (s, 6H); ^{13}C NMR (62.9 MHz, $CDCl_3$): $\delta = 175.1$ (C_0), 164.7 (C_0), 146.4 (C_0), 144.8 (C_0), 142.1 (CH), 136.0 (C_0), 134.1 (C_0), 132.0 (CH), 128.4 (2×CH), 127.8 (CH), 126.6 (CH), 126.4 (2×CH), 125.8 (CH), 121.3 (CH), 121.2 (CH), 120.7 (CH), 52.1 (CH), 41.0 (CH_2), 30.3 (CH_2), 29.6 (CH_2), 25.9 (6×CH_3), 18.3 (2×C_0), −4.2 (2×CH_3), −4.2 ppm (2×CH_3); HRMS (ESI+): *m/z* calcd for $C_{34}H_{50}NO_4Si_2$ [$M+H^+$]: 592.3278; found: 592.3361.

1-((*E*)-3-(4-(*tert*-Butyldimethylsilyloxy)-3-methoxyphenyl)acryloyl)-6-styryl-5,6-dihydropyridin-2(1*H*)-one (22): Prepared according to the general procedure for the N-acylation by using mixed anhydride and LHMDS in 77% yield (yellow solid). Eluent: hexanes/ethyl acetate, 3:1 *v/v*; mp: 145.0–147.0 °C; IR (thin film): $\tilde{\nu} = 2953$, 2934, 2893, 2860, 1686, 1508, 1396, 1339, 1285, 1256, 1198, 1162, 1036, 964, 918, 904, 840, 825, 781, 754, 696 cm^{-1}; ^1H NMR (250 MHz, $CDCl_3$): $\delta = 7.74$ (d, $J = 15.5$ Hz, 1H), 7.44 (d, $J = 15.5$ Hz, 1H), 7.37–7.18 (m, 5H), 7.14–7.04 (m, 2H), 6.84 (d, $J = 8.6$ Hz, 1H), 6.81–6.74 (m, 1H), 6.54 (d, $J = 16.0$ Hz, 1H), 6.23 (dd, $J = 16.0$, 5.8 Hz, 1H), 6.08 (dd, $J = 9.8$, 2.7 Hz, 1H), 5.61 (t, $J = 5.7$ Hz, 1H), 3.84 (s, 3H), 2.98–2.81 (m, 1H), 2.55 (dd, $J = 19.1$, 6.5 Hz, 1H), 1.00 (s, 9H), 0.17 ppm (s, 6H); ^{13}C NMR (62.9 MHz, $CDCl_3$): $\delta = 168.5$ (C_0), 165.4 (C_0), 151.1 (C_0), 147.4 (C_0), 144.4 (CH), 142.4 (CH), 136.1 (C_0), 132.0 (CH), 129.0 (C_0), 128.5 (2×CH), 127.8 (CH), 126.9 (CH), 126.5 (2×CH), 126.0 (CH), 122.6 (CH), 121.0 (CH), 119.5 (CH), 111.1 (CH), 55.4 (OCH_3), 52.8 (CH), 29.9 (CH_2), 25.6 (3×CH_3), 18.4 (C_0), −4.6 ppm (2×CH_3); HRMS (ESI+): *m/z* calcd for $C_{29}H_{36}NO_4Si$ [$M+H^+$]: 490.2414; found: 490.2460.

General procedure for the deprotection by using HF·pyridine: For the deprotection of the intermediates **20**–**22** containing a TBS group, a freshly prepared solution of HF·pyridine in anhydrous pyridine/anhydrous THF (27.0 mL of THF, 6.8 mL of pyridine, and 3.2 mL of HF·pyridine, 70:30) was added to a solution of the TBS-protected lactams (0.5 mmol) in anhydrous THF (3.0 mL), at 0 °C and under a nitrogen atmosphere. The resulting solution was maintained with magnetic stirring for 2 h, and after this period, a saturated aqueous solution of sodium hydrogen carbonate was added until pH ≈ 6 was reached (150 mL). The reaction mixture was extracted with ethyl acetate (3×70 mL), and the organic layer was washed with water (40 mL) and brine (40 mL), dried over anhydrous magnesium sulfate, filtered, and concentrated to dryness. The crude residue was purified by flash column chromatography (by using the indicated solvent) to give phenolic aza-goniothalamin analogues **23**–**25**.

1-((*E*)-3-(3,4-Dihydroxyphenyl)acryloyl)-6-styryl-5,6-dihydropyridin-2(1*H*)-one (23): Prepared according to the general procedure for the deprotection reaction by using hydrogen fluoride pyridine complex in 83% yield (yellow solid). Eluent: hexanes/ethyl acetate, 1:2 *v/v*; mp: 178.0–180.0 °C; IR (thin film): $\tilde{\nu} = 3330$, 1675, 1660, 1590, 1529, 1391, 1367, 1304, 1278, 1201, 1184, 1144, 1109, 1045, 966, 820, 742, 690 cm^{-1}; ^1H NMR (250 MHz, [D_6]acetone): $\delta = 8.28$ (br s, 1H), 7.60 (d, $J = 15.6$ Hz, 1H), 7.46–7.35 (m, 3H), 7.34–7.19 (m, 3H), 7.17 (d, $J = 1.8$ Hz, 1H), 7.03 (dd, $J = 8.2$, 1.8 Hz, 1H), 6.98–6.85 (m, 2H), 6.50 (d, $J = 16.0$ Hz, 1H), 6.37 (dd, $J = 16.0$, 5.0 Hz, 1H), 5.99 (dd, $J = 9.7$, 2.7 Hz, 1H), 5.55 (t, $J = 5.0$ Hz, 1H), 3.09–2.87 (m, 2H), 2.69 ppm (dd, $J = 18.7$, 6.1 Hz, 1H); ^{13}C NMR (62.9 MHz, [D_6]acetone): $\delta = 168.9$ (C_0), 166.2 (C_0), 148.6 (C_0), 146.3 (C_0), 144.4 (CH), 144.1 (CH), 137.5 (C_0), 131.9 (CH), 129.5 (2×CH), 129.2 (CH), 128.6 (CH), 127.3 (2×CH), 126.2 (CH), 122.7 (CH), 120.2 (CH), 116.5 (CH), 115.1 (CH), 53.7 (CH), 30.4 ppm (CH_2); HRMS (ESI+): *m/z* calcd for $C_{22}H_{20}NO_4$ [$M+H^+$]: 362.1392; found: 362.1457.

(*E*)-1-(3-(3,4-Dihydroxyphenyl)propanoyl)-6-styryl-5,6-dihydropyridin-2(1*H*)-one (24): Prepared according to the general procedure for the deprotection reaction by using hydrogen fluoride pyridine complex in 80% yield (white solid). Eluent: hexanes/ethyl acetate, 1:2 *v/v*; mp: 156.0–158.0 °C; IR (thin film): $\tilde{\nu} = 3500$, 3190, 1704, 1669, 1623, 1523, 1401, 1252, 1184, 1150, 1115, 827, 813, 739, 688 cm^{-1}; ^1H NMR (250 MHz, [D_6]acetone): $\delta = 7.66$ (s, 1H), 7.42–7.15 (m, 5H), 6.94–6.81 (m, 1H), 6.79–6.66 (m, 2H), 6.58 (dd, $J = 7.5$, 2.5 Hz, 1H), 6.45 (d, $J = 16.0$ Hz, 1H), 6.32 (dd, $J = 16.0$, 5.0 Hz, 1H), 5.94 (dd, $J = 10.0$, 2.5 Hz, 1H), 5.55 (t, $J = 5.0$ Hz, 1H), 3.36–3.03 (m, 2H), 2.97–2.76 (m, 3H), 2.63 ppm (dd, $J = 20.0$, 5.0 Hz, 1H); ^{13}C NMR (62.9 MHz, [D_6]acetone): $\delta = 175.6$ (C_0), 165.7 (C_0), 145.8 (C_0), 144.2 (CH), 137.5 (C_0), 134.0 (C_0), 131.9 (CH), 129.5 (2×CH), 129.0 (CH), 128.6 (CH), 127.3 (2×CH), 126.2 (CH), 120.6 (CH), 116.4 (CH), 116.1 (CH), 53.1 (CH), 42.0 (CH_2), 31.4 (CH_2), 29.3 ppm (CH_2); HRMS (ESI+): *m/z* calcd for $C_{22}H_{22}NO_4$ [$M+H^+$]: 364.1549; found: 364.1566.

1-((*E*)-3-(4-Hydroxy-3-methoxyphenyl)acryloyl)-6-styryl-5,6-dihydropyridin-2(1*H*)-one (25): Prepared according to the general procedure for the deprotection reaction by using hydrogen fluoride pyridine complex in 94% yield (yellow solid). Eluent: hexanes/ethyl acetate, 1:2 *v/v*; mp: 144.0–146.0 °C; IR (thin film): $\tilde{\nu} = 3303$, 1668, 1615, 1592, 1514, 1429, 1407, 1292, 1270, 1205, 1145, 1125, 1030, 999, 962, 826, 818, 741 cm^{-1}; ^1H NMR (250 MHz, $CDCl_3$): 7.74 (d, $J =$ 15.0 Hz, 1H), 7.44 (d, $J = 15.0$ Hz, 1H), 7.37–7.19 (m, 5H), 7.16–7.06 (m, 2H), 6.91 (d, $J = 7.5$ Hz, 1H), 6.86–6.74 (m,1H), 6.54 (d, $J =$ 16.0 Hz, 1H), 6.24 (dd, $J = 16.0$, 7.5 Hz, 1H), 6.14–5.99 (m, 2H), 5.61 (t, $J = 7.5$ Hz, 1H), 3.91 (s, 3H), 2.97–2.82 (m, 1H), 2.57 ppm (dd, $J =$ 17.5, 7.5 Hz, 1H); ^{13}C NMR (62.9 MHz, $CDCl_3$): $\delta = 168.5$ (C_0), 165.5 (C_0), 147.9 (C_0), 146.7 (C_0), 144.4 (CH), 142.5 (CH), 136.1 (C_0), 132.0 (CH), 128.5 (2×CH), 127.8 (CH), 127.7 (C_0), 126.9 (CH), 126.5 (2× CH), 125.9 (CH), 123.5 (CH), 119.1 (CH), 114.6 (CH), 109.6 (CH), 55.9 (OCH_3), 52.8 (CH), 29.9 ppm (CH_2); HRMS (ESI+): *m/z* calcd for $C_{23}H_{22}NO_4$ [$M+H^+$]: 376.1549; found: 376.1606.

Biological assays

In vitro assays

Cell lines: Human tumor U251 (glioma), MCF-7 (breast), NCI-H460 (lung, non-small cells), HT-29 (colon), PC-3 (prostate), 786–0

(kidney), NCI-ADR/RES (ovarian expressing multiple drugs resistance phenotype), and OVCAR-3 (ovary) cell lines were obtained from the National Cancer Institute at Frederick, MA, USA. The non-tumor HaCat (human keratinocytes) cell line was donated by Prof. Dr. Ricardo Della Coletta, FOP/UNICAMP.

Cell culture: Stock cultures were grown in Rosewell Park Memorial Institute (RPMI) 1640 medium (GIBCO BRL) supplemented with 5% fetal bovine serum (FBS; GIBCO), 100 U mL^{-1} penicillin, and 100 μg mL^{-1} streptomycin at 37 °C with 5% CO_2.

Antiproliferative assay: Cells in 96-well plates (100 μL cells/well) were exposed to goniothalamin (**1**), aza-goniothalamin (**2**), piplartine (**3**), or derivatives **13**–**19**, **23**–**25**, or **32**–**37** in concentrations of 0.25, 2.5, 25, and 250 μg mL^{-1} in DMSO/RPMI at 37 °C with 5% of CO_2 in air for 48 h. Doxorubicin was used as a positive control (0.025, 0.25, 2.5, and 25 μg mL^{-1}). The final DMSO concentration did not affect cell viability (0.1%). Afterwards, cells were fixed with 50% trichloroacetic acid, and cell proliferation was determined by spectrophotometric quantification (540 nm) of the cellular protein content by using the sulforhodamine B assay. The concentration that produces total growth inhibition or cytostatic effect (TGI value) was determined through nonlinear regression analysis by using the concentration-response curve for each cell line in ORIGIN 8.0 software (OriginLab Corporation). The results were expressed in μM as the mean ± the standard deviation.[16a,b,49]

Measurement of intracellular ROS production: Intracellular ROS levels were measured by flow cytometry in cells loaded with the redox-sensitive dye DCFH-DA (Sigma). Briefly, PC-3 cells were washed with Hank's buffered salt solution (HBSS) medium and incubated in the dark for 30 min at 37 °C with 10 μM DCFH-DA. The cells were then treated with **1** (20 μM), **2** (20 μM), and **18** (5 and 10 μM). After 1 h of treatment, cells were harvested and resuspended in the HBSS medium. Fluorescence was recorded on the FL-1 channel of a Guava Easycyte Mini flow cytometer (Guava Technologies, Hayward, CA). The data were analyzed with the CytoSoft 4.1 software in the Guava Express Pro program.

Measurement of phosphatidylserine externalization: Phosphatidylserine externalization was analyzed by using a Guava Nexin assay kit (Guava Technologies, Hayward, CA) in accordance with the manufacturer's instructions. PC-3 cells were treated with **1** (20 μM), **2** (20 μM), and **18** (5 and 10 μM) for 6, 15, 18, and 24 h. The cells were then harvested and resuspended at a density of 1×10^5 cells in 100 μL of supplemented medium. Binding buffer (100 mL) containing Annexin V and 7-AAD was added to the cells and the reaction was incubated in the dark for 20 min at room temperature. The cells were then analyzed with a Guava Easycyte Mini flow cytometer (Guava Technologies, Hayward, CA).

Measurement of multicaspase activation: Multicaspase activation was analyzed by using a Guava Multicaspase assay kit (Guava Technologies, Hayward, CA) in accordance with the manufacturer's instructions. PC-3 cells were treated with **1** (20 μM), **2** (20 μM), and **18** (5 and 10 μM) for 18 and/or 24 h. Cells were harvested and resuspended at a density of 1×10^5 cells, and binding buffer containing sulforhodamine-valyl-alanyl-aspartyl-fluoromethylketone (SR-VAD-FMK) was added to the cells (100 μL). The suspension was incubated in the dark for 60 min at room temperature. After washing and centrifugation cycles, the cells were incubated in 7-AAD buffer for 10 min and analyzed with a Guava Easycyte Mini flow cytometer (Guava Technologies, Hayward, CA).

Cell-cycle analyses: Cells cycle analyses were performed with the Guava Cell Cycle reagent (Guava Technologies, Hayward, CA) in accordance with the manufacturer's instructions. PC-3 cells were deprived for 24 h and then treated with **1** (10 μM), **2** (20 μM), and **18** (5 μM) for 24 h. The cells were then harvested and resuspended at a density of 1×10^5 cells in phosphate-buffered saline (PBS; 100 μL). The binding buffer containing propidium iodide (PI) was added to the cells (100 μL), and the suspension was incubated in the dark for 20 min at room temperature. The cells were then analyzed with a Guava Easycyte Mini flow cytometer (Guava Technologies, Hayward, CA).

In vivo assays

Animals: Experiments were conducted with Balb/C female mice (20–30 g, 90 days old) from the Multidisciplinary Center for Biological Investigation on Laboratory Animals Sciences (CEMIB-UNICAMP. Animals were maintained at the Animal Facilities of the Pharmacology and Toxicology Division, CPQBA, UNICAMP (Campinas, Brazil), in a room with a controlled temperature of (25 ± 2) °C for a 12 h light/dark cycle, with free access to food and water. Animal care and research protocols were in accordance with the principles and guidelines adopted by the Brazilian College of Animal Experimentation (COBEA). Protocols were approved by the Ethical Committee for Animal Research (3432–1), Institute of Biology, UNICAMP.

Acute toxicity: Balb/C mice were treated intraperitoneally (i.p.) with **2** and **18** (50, 100, and 150 mg kg^{-1} for compound **18** and 50, 100, 300, 600, and 1000 mg kg^{-1} for compound **2**). Groups were observed for 4 h and then daily for 15 days. The following parameters were evaluated: general toxicity signals like body weight loss, locomotion, behavior (agitation, lethargy), respiration, salivation, tearing eyes, cyanosis, and mortality.[50] Goniothalamin (**1**) acute toxicity was already evaluated in a previous study.[6e]

Ehrlich ascitic and solid tumors in mice

Cell maintenance and preparation: Ehrlich tumor cells were maintained in the ascitic form by peritoneal passages in mice by weekly transplantation of 5×10^5 tumor cells/animal in PBS.[51] For the tests, cells were prepared at the proper density in PBS (1.0×10^4 cells/100 μL/animal for ascitic tumors and 10×10^6 cells/60 μL/animal for solid tumors).[52] Cells were centrifuged and resuspended in PBS for counting in a Neubauer chamber with trypan blue, to exclude nonviable cells and debris.

Ehrlich ascitic tumor: Balb/C mice ($n=8$ per group) were inoculated in the peritoneum with Ehrlich cells (1.0×10^4 cells/100 μL/animal). After 48 h, the animals were divided into groups and treated every day, i.p. for five days, as negative control (vehicle, PBS + Tween 80), positive control (5-FU; 10 mg kg^{-1}), and experimental groups (**1**, **2**, or **18**; 50 mg kg^{-1}). On eighth day of the experiment, the animals were euthanized by using an overdose of anesthetic, and ascites were collected after injection of 3 mL of PBS into the peritoneum. The obtained suspension was centrifuged for 5 min at 2500 rpm and 4 °C, the supernatant was again discarded, and the cell pellet was resuspended in PBS at a ratio of 1:20. The number of cells/mL was determined by flow cytometry (Guava EasyCite MiniSystem Millipore), excluding cell debris and small sized cells.[53]

Ehrlich solid tumor: Balb/C mice ($n=8$/group) were inoculated in the subcutaneum with Ehrlich cells (10×10^6 cells/60 μL/animal).[54] When tumors were palpable (5 days later), the animals were divided into groups and treated every day, i.p. for 15 days, as negative control (vehicle, PBS + Tween 80), positive control (5-FU; 10 mg kg^{-1}), and experimental groups (**1**, **2**, or **18**; 30, 30, and 40 mg kg^{-1}, respectively). On twentieth day of the experiment, the

animals were euthanized by using an overdose of anesthetic. The tumors were removed and weighed, and the growth inhibition ratio was calculated according to the formula: $[(A-B)/A]\times 100$, in which A is the mean of the control-group tumor weight and B is the mean of the treated-group tumor weight. The relative tumor weight was also calculated, as tumor weight divided by corporal weight.[55]

At the end of the experiment, the hemogram was analyzed from the whole blood of the animals (Sysmex model Poch-100iV), and the total leukocytes (WBC), erythrocytes (RBC), hemoglobin (Hbg), and platelets (Pt) were evaluated. The lungs, heart, liver, spleen, and kidneys were also removed and weighed. Only modified parameters have been presented.

Statistical analyses

GraphPad Prism 5.0 software was used for statistical analyses. The results are shown as the mean ± standard error of mean (SEM). The statistical significance of difference between the groups was assessed by one-way ANOVA, followed by Tukey's post hoc test. Values of $p > 0.05$ were considered significant.

Supporting Information

The Supporting Information contains the ^{1}H and ^{13}C NMR spectra for compounds **3**, **8**, **9**, **12**–**25**, and **32**–**37**, the method of preparation and the ^{1}H and ^{13}C NMR spectra for some of the carboxylic acids used in the N-acylation reaction, the ^{1}H NMR spectra for the study of GSH addition to compounds **1**, **2**, **3**, and **18**, and the concentration–response curves for doxorubicin and compounds **1**–**3**, **13**–**19**, **23**–**25**, and **32**–**39** and Figure S103.

Acknowledgements

The authors thank the São Paulo Research Foundation—FAPESP (grants 2009/51602-5, 2012/18281-3, and 2010/16990-1), CNPq, and Capes for financial support, and the National Cancer Institute (Frederick, MD, USA) for granting the human tumor cell lines. We also thank Prof. Edilberto Rocha Silveira from the Federal University of Ceará for providing us with an authentic sample of piplartine. The manuscript was written through contributions from all authors. All authors have given approval to the final version of the manuscript. The authors declare no competing financial interest.

Keywords: acylation · antitumor agents · aza compounds · cytotoxicity · goniothalamin

[1] National Cancer Institute, USA, http://www.cancer.gov, **2014** (accessed June 2014).
[2] J. Ferlay, I. Soerjomataram, M. Ervik, R. Dikshit, S. Eser, C. Mathers, M. Rebelo, D. M. Parkin, D. Forman, F. Bray, International Agency for Research on Cancer: GLOBOCAN 2012 1.0, http://globocan.iarc.fr, **2013** (accessed June 2014).
[3] D. B. Longley, P. G. Johnston, *J. Pathol.* **2005**, *205*, 275 – 292.
[4] D. J. Newman, G. M. Cragg, *J. Nat. Prod.* **2012**, *75*, 311 – 335.
[5] G. M. Cragg, D. J. Newman, *Phytochem. Rev.* **2009**, *8*, 313 – 331.
[6] a) A. de Fátima, L. K. Kohn, M. A. Antônio, J. E. de Carvalho, R. A. Pilli, *Bioorg. Med. Chem.* **2005**, *13*, 2927 – 2933; b) A. de Fátima, L. K. Kohn, J. E. Carvalho, R. A. Pilli, *Bioorg. Med. Chem.* **2006**, *14*, 622 – 6531; c) C. C. Chiu, P. L. Liu, K. J. Huang, H. M. Wang, K. F. Chang, C. K. Chou, F. R. Chang, I. W. Chong, K. Fang, J. S. Chen, H. W. Chang, Y- C. Wu, *J. Agric. Food Chem.* **2011**, *59*, 4288 – 4293; d) M. Al-Qubaisi, R. Rozita, S.-K. Yeap, A.-R. Omar, A.-M. Ali, N. B. Alitheen, *Molecules* **2011**, *16*, 2944 – 2959; e) D. B. Vendramini-Costa, I. B. D. de Castro, A. L. T. G. Ruiz, C. Marquissolo, R. A. Pilli, J. E. de Carvalho, *Bioorg. Med. Chem.* **2010**, *18*, 6742 – 6747.
[7] a) S. H. Inayat-Hussain, B. O. Annuar, L. B. Din, A. M. Ali, D. Ross, *Toxicol. In Vitro* **2003**, *17*, 433 – 439; b) S. H. Inayat-Hussain, A. B. Osman, L. B. Din, A. M. Ali, R. T. Snowden, M. MacFarlane, K. Cain, *FEBS Lett.* **1999**, *456*, 379 – 383; c) A. de Fátima, W. F. Zambuzzi, L. V. Modolo, C. A. B. Tarsitano, F. R. Gadelha, S. Hylsop, J. E. de Carvalho, I. Salgado, C. V. Ferreira, R. A. Pilli, *Chem.-Biol. Interact.* **2008**, *176*, 143 – 150; d) J.-Y. Wach, S. Güttinger, U. Kutay, K. Gademann, *Bioorg. Med. Chem. Lett.* **2010**, *20*, 2843 – 2846; e) F. S. Zhou, W. D. Tang, Q. Mu, G. X. Yang, Y. Wang, G. L. Liang, L. G. Lou, *Chem. Pharm. Bull.* **2005**, *53*, 1387 – 1391; f) P. Kasaplar, Ö. Yilmazer, A. Çağir, *Bioorg. Med. Chem.* **2009**, *17*, 311 – 318; g) R. C. Barcelos, J. C. Pastre, V. Caixeta, D. B. Vendramini-Costa, J. E. de Carvalho, R. A. Pilli, *Bioorg. Med. Chem.* **2012**, *20*, 3635 – 3651; h) M. Bruder, D. B. Vendramini-Costa, J. E. de Carvalho, R. A. Pilli, *Bioorg. Med. Chem.* **2013**, *21*, 5107 – 5117.
[8] a) L. Bialy, H. Waldmann, *Chem. Commun.* **2003**, 1872 – 1873; b) S. B. Buck, C. Hardouin, S. Ichikawa, D. R. Soenen, C.-M. Gauss, I. Hwang, M. R. Swingle, K. M. Bonness, R. E. Honkanen, D. L. Boger, *J. Am. Chem. Soc.* **2003**, *125*, 15694 – 15695.
[9] Q.-X. Yue, X. Liu, D.-A. Guo, *Planta Med.* **2010**, *76*, 1037 – 1043.
[10] a) D. P. Bezerra, F. O. Castro, A. P. N. N. Alves, C. Pessoa, M. O. Moraes, E. R. Silveira, M. A. S. Lima, F. J. M. Elmiro, N. M. N. Alencar, R. O. Mesquita, M. W. Lima, L. V. Costa-Lotufo, *J. Appl. Toxicol.* **2008**, *28*, 156 – 163; b) L. Raj, T. Ide, A. U. Gurkar, M. Foley, M. Schenone, X. Li, N. J. Tolliday, T. R. Golub, S. A. Carr, A. F. Shamji, A. M. Stern, A. Mandinova, S. L. Schreiber, S. W. Lee, *Nature* **2011**, *475*, 231 – 234.
[11] S.-S. Han, V. S. Tompkins, D. J. Son, N. L. Kamberos, L. L. Stunz, A. Halwani, G. A. Bishop, S. Janz, *Biochem. Biophys. Res. Commun.* **2013**, *436*, 660 – 665.
[12] P. Makhov, K. Golovine, E. Teper, A. Kutikov, R. Mehrazin, A. Corcoran, A. Tulin, R. G. Uzzo, *Br. J. Cancer* **2014**, *110*, 899 – 907.
[13] D. P. Bezerra, C. Pessoa, M. O. de Moraes, N. Saker-Neto, E. R. Silveira, L. V. Costa-Lotufo, *Eur. J. Pharm. Sci.* **2013**, *48*, 453 – 463.
[14] J. McNulty, J. A. Steere, S. Wolf, *Tetrahedron Lett.* **1998**, *39*, 8013 – 8016.
[15] P. M. Boll, J. Hansen, O. Simonsen, N. Thorup, *Tetrahedron* **1984**, *40*, 171 – 175.
[16] a) A. Monks, D. Scudiero, P. Skehan, R. Shoemaker, K. Paull, D. Vistica, C. Hose, J. Langley, P. Cronise, A. Vaigro-Wolff, M. Gray-Goodrich, H. Campbell, J. Mayo, M. Boyd, *J. Nat. Cancer Inst.* **1991**, *83*, 757 – 766; b) R. H. Shoemaker, *Nat. Rev. Cancer* **2006**, *6*, 813 – 823.
[17] A. de Fátima, L. V. Modolo, L. S. Conegero, R. A. Pilli, C. V. Ferreira, L. K. Kohn, J. E. de Carvalho, *Curr. Med. Chem.* **2006**, *13*, 3371 – 3384.
[18] M. Hagel, D. Niu, T. St. Martin, M. P. Sheets, L. Qiao, H. Bernard, R. M. Karp, Z. Zhu, M. T. Labenski, P. Chaturvedi, M. Nacht, W. F. Westlin, R. C. Petter, J. Singh, *Nat. Chem. Biol.* **2011**, *7*, 22 – 24.
[19] I. M. Serafimova, M. A. Pufall, S. Krishnan, K. Duda, M. S. Cohen, R. L. Maglathlin, J. M. McFarland, R. M. Miller, M. Frödin, J. Taunton, *Nat. Chem. Biol.* **2012**, *8*, 471 – 476.
[20] D. J. Adams, Z. V. Boskovic, J. R. Theriault, A. J. Wang, A. M. Stern, B. K. Wagner, A. F. Shamji, S. L. Schreiber, *ACS Chem. Biol.* **2013**, *8*, 923 – 929.
[21] a) C. A. Gomes, T. G. Da Cruz, J. L. Andrade, N. Milhazes, F. Borges, M. P. M. Marques, *J. Med. Chem.* **2003**, *46*, 5395 – 5401; b) T. W. Chung, S. K. Moon, Y. C. Chang, J. H. Ko, Y. C. Lee, G. Cho, S. H. Kim, J. G. Kim, C. H. Kim, *FASEB J.* **2004**, *18*, 1670 – 1681; c) H. F. Liao, Y. Y. Chen, J. J. Liu, M. L. Hsu, H. J. Shieh, H. J. Liao, C. J. Shieh, M. S. Shiao, Y. J. Chen, *J. Agric. Food Chem.* **2003**, *51*, 7907 – 7912.
[22] J. E. Jung, H. S. Kim, C. S. Lee, D. H. Park, Y. N. Kim, M. J. Lee, J. W. Lee, J. W. Park, M. S. Kim, S. K. Ye, M. H. Chung, *Carcinogenesis* **2007**, *28*, 1780 – 1787.
[23] T. Karantanos, P. G. Corn, T. C. Thompson, *Oncogene* **2013**, *32*, 5501 – 5511.
[24] T. Vanden Berghe, S. Grootjans, V. Goossens, Y. Dondelinger, D. V. Krysko, N. Takahashi, P. Vandenabeele, *Methods* **2013**, *61*, 117 – 129.
[25] R. S. Wong, *J. Exp. Clin. Cancer Res.* **2011**, *30*, 87.
[26] K.-Y. Kim, Y.-K. Seo, S.-N. Yu, S.-H. Kim, P.-G. Suh, J.-H. Ji, H.-S. Yu, Y.-M. Park, S.-C. Ahn, *J. Cancer Sci. Ther.* **2013**, *5*, 023 – 030.
[27] G. H. Williams, K. Stoeber, *J. Pathol.* **2012**, *226*, 352 – 364.

[28] a) D. Hanahan, R. A. Weinberg, *Cell* **2011**, *144*, 646 – 674; b) A. P. Demchenko, *Cytotechnology* **2013**, *65*, 157 – 172.
[29] a) D. Trachootham, Y. Zhou, H. Zhang, Y. Demizu, Z. Chen, H. Pelicano, P. J. Chiao, G. Achanta, R. B. Arlinghaus, J. Liu, P. Huang, *Cancer Cell* **2006**, *10*, 241 – 252; b) M. L. Guzman, R. M. Rossi, S. Neelakantan, X. Li, C. A. Corbett, D. C. Hassane, M. W. Becker, J. M. Bennett, E. Sullivan, J. L. Lachowicz, A. Vaughan, C. J. Sweeney, W. Matthews, M. Carroll, J. L. Liesveld, P. A. Crooks, C. T. Jordan, *Blood* **2007**, *110*, 4427 – 4435; c) S. Dolma, S. L. Lessnick, W. C. Hahn, B. R. Stockwell, *Cancer Cell* **2003**, *3*, 285 – 296; d) A. T. Shaw, M. M. Winslow, M. Magendantz, C. Ouyang, J. Dowdle, A. Subramanian, T. A. Lewis, R. L. Maglathin, N. Tolliday, T. Jacks, *Proc. Natl. Acad. Sci. USA* **2011**, *108*, 8773 – 8778.
[30] D. Trachootham, J. Alexandre, P. Huang, *Nat. Rev. Drug Discovery* **2009**, *8*, 579 – 591.
[31] L. A. Sena, N. S. Chandel, *Mol. Cell* **2012**, *48*, 158 – 167.
[32] P. T. Schumacker, *Cancer Cell* **2006**, *10*, 175 – 176.
[33] K. M. Chan, N. F. Rajab, M. H. A. Ishak, A. M. Ali, K. Yusoff, L. B. Din, S. H. Inayat-Hussain, *Chem.-Biol. Interact.* **2006**, *159*, 129 – 140.
[34] W. Y. Chen, C. C. Wu, Y. H. Lan, F. R. Chang, C. M. Teng, Y. C. Wu, *Eur. J. Pharmacol.* **2005**, *522*, 20 – 29.
[35] a) S. H. Inayat-Hussain, K. M. Chan, N. F. Rajab, L. B. Din, S. C. Chow, A. Kizilors, F. Farzaneh, G. T. Williams, *Toxicol. Lett.* **2010**, *193*, 108 – 114; b) C. Y. Yen, C. C. Chiu, R. W. Haung, C. C. Yeh, K. J. Huang, K. F. Chang, Y. C. Hseu, F. R. Chang, H. W. Chang, Y. C. Wu, *Mutat. Res.* **2012**, *747*, 253 – 258.
[36] G. K. Balendiran, R. Dabur, D. Fraser, *Cell Biochem. Funct.* **2004**, *22*, 343 – 352.
[37] S. Reuter, S. C. Gupta, M. M. Chaturvedi, B. B. Aggarwal, *Free Radical Biol. Med.* **2010**, *49*, 1603 – 1616.
[38] D. J. Adams, M. Dai, G. Pellegrino, B. K. Wagner, A. M. Stern, A. F. Shamji, S. L. Schreiber, *Proc. Natl. Acad. Sci. USA* **2012**, *109*, 15115 – 15120.
[39] a) T. J. Schmidt, *Bioorg. Med. Chem.* **1997**, *5*, 645 – 653; b) T. J. Schmidt, G. Lyß, H. L. Pahl, I. Merfort, *Bioorg. Med. Chem.* **1999**, *7*, 2849 – 2855; c) J. Heilmann, M. R. Wasescha, T. J. Schmidt, *Bioorg. Med. Chem.* **2001**, *9*, 2189 – 2194; d) P. A. Whitton, A. Lau, A. Salisbury, J. Whitehouse, C. S. Evans, *Phytochemistry* **2003**, *64*, 673 – 679; e) E. Butturini, E. Cavalieri, A. C. De Prati, E. Darra, A. Rigo, K. Shoji, N. Murayama, H. Yamazaki, Y. Watanabe, H. Suzuki, S. Mariotto, *PLoS One* **2011**, *6*, e20174.
[40] a) A. E. Mitchell, J. Zheng, B. D. Hammock, M. L. Bello, A. D. Jones, *Biochemistry* **1998**, *37*, 6752 – 6759; b) J. Zheng, A. E. Mitchell, A. D. Jones, B. D. Hammock, *J. Biol. Chem.* **1996**, *271*, 20421 – 20425.
[41] J. M. Matés, J. A. Segura, F. J. Alonso, J. Márquez, *Arch. Toxicol.* **2012**, *86*, 1649 – 1665.
[42] M. L. Circu, T. Y. Aw, *Free Radical Biol. Med.* **2010**, *48*, 749 – 762.
[43] H. L. Stewart, *Cancer Res.* **1959**, *19*, 804 – 818.
[44] R. A. Weinberg, *The biology of cancer*, 1edst edGarland Science, New York, **2006**, p. 850.
[45] O. Tredan, C. M. Galmarini, K. Patel, I. F. Tannock, *J. Natl. Cancer Inst.* **2007**, *99*, 1441 – 1454.
[46] C. Bincoletto, S. Eberlin, C. A. Figueiredo, M. B. Luengo, M. L. Queiroz, *Int. Immunopharmacol.* **2005**, *5*, 679 – 688.
[47] Y. Pommier, *Nat. Rev. Cancer* **2006**, *6*, 789 – 802.
[48] R. C. Pandey, M. W. Toussaint, R. M. Stroshane, C. C. Kalita, A. A. Aszalos, A. L. Garretson, T. T. Wei, K. M. Byrne, R. F. Geoghegan, Jr., R. J. White, *J. Antibiot.* **1981**, *34*, 1389 – 1401.
[49] P. Skehan, R. Storeng, D. Scudiero, A. Monks, J. McMahon, D. Vistica, J. T. Warren, H. Bokesch, M. R. Boyd, *J. Natl. Cancer Inst.* **1990**, *82*, 1107 – 1112.
[50] J. T. Litchfield Jr., F. Wilcoxon, *J. Pharmacol. Exp. Ther.* **1949**, *96*, 99 – 113.
[51] a) S. C. Salgado Oloris, M. L. Z. Dagli, J. L. Guerra, *Life Sci.* **2002**, *71*, 717 – 724; b) F. R. F. Nascimento, G. V. B. Cruz, P. V. S. Pereira, M. C. G. Maciel, L. A. Silva, A. P. S. Azevedo, E. S. B. Barroqueiro, R. N. M. Guerra, *Life Sci.* **2006**, *78*, 2650 – 2653; c) N. M. Gomes, C. M. Rezende, S. P. Fontes, A. M. C. Hovell, R. G. Landgraf, M. E. Matheus, A. C. Pinto, P. D. Fernandes, *J. Ethnopharmacol.* **2008**, *119*, 179 – 184.
[52] a) J. L. Sacoman, K. M. Monteiro, A. Possenti, G. M. Figueira, M. A. Foglio, J. E. Carvalho, *Braz. J. Med. Biol. Res.* **2008**, *41*, 411 – 415; b) I. F. Tannock, *Cancer Res.* **1969**, *29*, 1527 – 1534.
[53] L. Ray, P. Kumar, K. C. Gupta, *Biomaterials* **2013**, *34*, 3064 – 3076.
[54] M. A. El-Sayed, A. A. Shabaka, O. A. El-Shabrawy, N. A. Yassin, S. S. Mahmoud, S. M. El-Shenawy, E. Al-Ashqar, W. H. Weisa, N. M. Farag, M. A. El-Shaer, N. Salah, A. M. Al-Abd, *PloS one* **2013**, *8*, e76207.
[55] D. P. Bezerra, F. O. Castro, A. P. N. N. Alves, C. Pessoa, M. O. Moraes, E. R. Silveira, M. A. S. Lima, F. J. M. Elmiro, L. V. Costa-Lotufo, *Braz. J. Med. Biol. Res.* **2006**, *39*, 801 – 807.

Received: July 16, 2014
Published online on ■■ ■■, 0000

*R. C. Barcelos, J. C. Pastre, D. B. Vendramini-Costa, V. Caixeta, G. B. Longato, P. A. Monteiro, J. E. de Carvalho, R. A. Pilli**

■■ – ■■

Design and Synthesis of N-Acylated Aza-Goniothalamin Derivatives and Evaluation of Their in vitro and in vivo Antitumor Activity

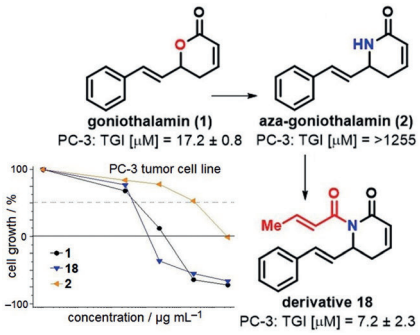

In vivo l'importance! We conducted antiproliferation assays of a library of aza derivatives of goniothalamin (**1**) against a panel of tumor cell lines. The most potent compound, **18**, led to reactive oxygen species generation, apoptosis, and G_2/M cell-cycle arrest in prostate PC-3 cells, but it failed to inhibit tumor growth. Surprisingly, aza-goniothalamin (**2**), which was shown to be much less toxic in vitro, inhibited Ehrlich tumor development in mice.